C.P. No. 1346

C.P. No. 1346

PROCUREMENT EXECUTIVE, MINISTRY OF DEFENCE

AERONAUTICAL RESEARCH COUNCIL

CURRENT PAPERS

Measurement of the Internal Performance of a Rectangular Air-Intake at a Mach Number of 0.9

by

C. S. Brown and E. L. Goldsmith

Aerodynamics Dept., R.A.E., Bedford

LONDON: HER MAJESTY'S STATIONERY OFFICE

1976

UDC 533.697.24 : 532.542.1 : 533.6.011.35

*CP No.1346
January, 1973

MEASUREMENT OF THE INTERNAL PERFORMANCE OF A RECTANGULAR AIR-INTAKE AT A MACH NUMBER OF 0.9

by

C. S. Brown
E. L. Goldsmith

SUMMARY

A rectangular intake having variable geometry compression surfaces and designed for supersonic operation has been tested at a Mach number of 0.9 and a Reynolds number based on intake entry height of approximately 10^6. Tests have been made on the intake in isolation and on the side of a fuselage.

Maximum mass flow is less than estimates based on geometric throat size. The deficit corresponds to an effective reduction in throat area of about 3 per cent. Critical point pressure recovery is lower than predicted, but the difference can be related to a 'turning loss' factor as was the case at supersonic speeds.

With the compression surfaces of the intake horizontal, performance was unaffected by angle of incidence within the range 0° to 10°. With the compression surfaces vertical however, there was some loss in maximum mass flow and pressure recovery at critical flow conditions at angles of incidence above about 4°. This was only partly alleviated by removal of the swept endwalls.

The presence of this particular fuselage imposed no obvious effect on the performance of the intake.

---

* Replaces RAE Technical Report 73020 - ARC 34702.

CONTENTS

1 INTRODUCTION

An extensive programme of wind-tunnel tests has been carried out at RAE, Bedford to investigate the internal performance of a particular rectangular intake both in a uniform flow field and on a fuselage.

Details of the supersonic performance at Mach numbers between 1.6 and 2.5 are contained in Refs.1, 2 and 3. This Report presents the results from tests made on the same intake at a Mach number of 0.9. Tests have been made on the intake in isolation and also when installed on the side of a fuselage forebody with the compression surfaces of the intake both horizontal and vertical. In the case of the vertical intake the effect of removing the swept endwalls was investigated.

2 DESCRIPTION OF THE TEST RIG

Figs.1 and 2 show the intake, duct and forebody assembled on the General Intake Test Rig used in the 3ft wind tunnel at RAE, Bedford. This rig has been described in Ref.4. It consists of a sting support, a calibrated mass flow control and measuring unit, a hydraulic actuator system for moving the intake compression surface ramps and an instrumented duct with interchangeable exit plugs for controlling and measuring the intake bleed flow.

3 DETAILS OF THE MODEL

The intake is designed for supersonic operation and the model is that used in Refs.1, 2 and 3. The ratio of height to width at the entry plane is 1.54 and the geometry of the compression surface ramps, cowl and bleed are as shown in Fig.3. The first compression surface has a fixed angle δ_1 of 10° and the shock from the leading edge theoretically falls on the cowl lip at a free stream Mach number of 2.43. The second compression surface is movable and is linked to the rear ramp. In the configuration in which the intake is mounted on the fuselage with its leading edge vertical, the two movable surfaces are connected to the hydraulic actuator system on the intake test rig. However, when the intake is assembled on the fuselage so that its leading edge is horizontal this arrangement is not possible and the movable surfaces although still linked together in the manner shown in Fig.3, are controlled by means of a manually operated lead screw.

The gap between the second and rear ramps forms a slot for bleeding the boundary layer from the compression surfaces and this slot extends the whole width of the intake. The bleed air is discharged through a duct into the free stream. Bleed exit area is varied by means of interchangeable plugs. In addition to zero bleed, tests were done at constant ratios of bleed exit area to intake entry area of 0.05, 0.101 and 0.174.

Two different shapes of endwall were used in these tests. One was a full swept endwall in which the leading edge coincides with the line joining the leading edge of the intake to the cowl lip. The other is a minimal endwall which is sufficient to contain the space under the second ramp at maximum δ_2, but otherwise has a leading edge which is vertical at the cowl lip. Details of the two shapes are shown in Fig.4.

The area distribution through the intake and duct for various values of δ_2 is shown in Fig.5a while Fig.5b shows the area distribution through the intake alone between the cowl lip and the rear hinge for those values of δ_2 used in the tests. The ratio of engine face cross-sectional area to maximum intake capture area is 0.88 and the distance from the cowl lip to the engine face is 9.89 times the intake height.

The nose and canopy only of the fuselage are represented. Fig.6 shows details of the forebody including the relationship between the fuselage datum, the intake datum and the nose cone centre line. The model is mounted in the tunnel on the intake datum line so that α is the angle of incidence of the intake relative to the wind-tunnel free stream.

4 DETAILS OF THE TESTS

4.1 Test conditions

The tests were all made in the 3ft wind tunnel at RAE, Bedford, utilising the working section with top and bottom slotted walls. Tunnel conditions were such as would give a free stream Mach number of 0.90 in the empty tunnel. The effect on free stream Mach number of the intake test rig which has the rather high blockage ratio of about 3 per cent is not known and no corrections for wall constraint have been applied. The Reynolds number based on entry height was approximately 10^6.

4.2 Instrumentation and data reduction

The standard mass-flow control and measuring unit used in these tests is fitted with a cruciform rake having a total of 24 pitot tubes for measuring total pressure at the engine face station. The tubes are disposed for area-weighted averaging and the rake is rotatable to enable pressure surveys to be made in greater detail. Static pressure at the engine face is measured by using four holes equally spaced around the circumference. Details of the characteristics and calibration of this type of airflow meter are to be found in Ref.5.

The bleed duct contains twelve pitot tubes arranged in three rakes of four tubes for measuring total pressure and three holes for measuring static pressure.

Pressure recovery is defined as:-

$$\frac{P_f}{P_\infty} \quad \text{or} \quad \frac{P_B}{P_\infty} = \frac{1}{nP_\infty} \sum_{1}^{n} P_j \tag{1}$$

where P_∞ is the free stream total pressure and P_j is the pitot pressure at the jth tube in the rake at the engine face station in the case of P_f or in the rake in the bleed duct in the case of P_B; and n is in either case the number of pressure points in the survey.

The ratio of engine face mass flow to maximum capture flow was computed from:-

$$\left(\frac{A_\infty}{A_e}\right)_f = \frac{K_f A_f}{nA_e} \frac{\sum_{1}^{n} \frac{P_j}{P_\infty} \frac{M_j}{\left(1 + 0.2M_j^2\right)^3}}{\frac{M_\infty}{\left(1 + 0.2M_\infty^2\right)^3}} \tag{2}$$

where M_j = local Mach number calculated from P_j and p_f; p_f being the average static pressure at the engine face

A_e = maximum capture area

A_f = area at the engine face

K_f = discharge coefficient obtained by calibration[5].

Similarly bleed mass flow ratio was computed from:-

$$\left(\frac{A_\infty}{A_e}\right)_B = \frac{A_D}{nA_e} \frac{\sum_{1}^{n} \frac{P_j}{P_\infty} \frac{M_j}{\left(1 + 0.2M_j^2\right)^3}}{\frac{M_\infty}{\left(1 + 0.2M_\infty^2\right)^3}} \tag{3}$$

where P_j now refers to pressures in the bleed duct and M_j is the local Mach number calculated from P_j and p_B, the average static pressure in the bleed duct. A_D is the area of the bleed duct, in this case used without a discharge coefficient.

Total mass flow ratio

$$\left(\frac{A_\infty}{A_e}\right)_T = \left(\frac{A_\infty}{A_e}\right)_f + \left(\frac{A_\infty}{A_e}\right)_B \quad . \tag{4}$$

The parameter used to define flow distortion at the engine face is DC_{60}, defined as

$$DC_{60} = \frac{\left(\bar{P}_{60} - P_f\right)}{q_f} \tag{5}$$

where $\bar{P}_{60}$ is the mean total pressure in the worst 60^o sector and q_f is the mean dynamic pressure at the engine face, derived from P_f and p_f.

4.3 Accuracy

Errors in the direct measurement of engine face and bleed duct total pressure and therefore in pressure recoveries based on free stream total pressure are thought to be small, not more than 0.1 per cent. Uncertainty associated with the mean tunnel Mach number and more particularly with the calibration of the airflow meter probably means that the error in mass flow ratio could be as much as half a per cent.

5 DISCUSSION OF RESULTS

5.1 Isolated intake

Figs.7, 8 and 9 show the internal performance of the isolated intake at three different values of bleed exit area, including the case of zero bleed, and for a range of values of second ramp angle δ_2. Pitching the intake with its compression surfaces horizontal had no effect on the pressure recovery - mass flow characteristics within the range of incidence investigated.

Fig.10 summarises the variation with bleed exit area of maximum total and maximum engine face mass flow, maximum pressure recovery and critical point pressure recovery. The effect on performance of internal contraction in the duct and of the location of the throat in the duct is well illustrated. At values of second ramp angle δ_2 above about 5^o where the minimum duct area is in the region of the bleed slot, the bleed becomes inoperative at maximum mass flow owing to the low internal pressure.

At values of δ_2 between 2^o and 5^o it is possible to obtain small amounts of bleed flow but as bleed exit area is increased the intake soon chokes in the region of the bleed slot. At values of δ_2 below 2^o the minimum duct area is at the rear hinge and bleed mass flow increases quite normally with increasing bleed exit area. For all values of δ_2 maximum engine face mass flow is practically independent of bleed exit area. For values of δ_2 above about 2^o the large bleed exit area $(A_B/A_e) = 0.10$ results in a slight reduction in maximum mass flow. This is not clearly understood.

The apparent minimum duct area has been derived from measured maximum mass flow and is shown in Fig.11, together with the geometric minimum duct area and the inlet entry area at the cowl lip. The ratio of apparent to geometric minimum duct area is approximately 0.97 except when the throat is at the rear hinge, in which case the ratio falls to a minimum of 0.955.

Critical point pressure recovery shows a very slight increase with increasing bleed exit area (Fig.10). This occurs with or without bleed flow except at δ_2 equal to 0^o where with a large bleed flow pressure recovery falls off by about 2 per cent. Estimates of skin friction and interference losses based on the work of Ref.6 indicate that at critical flow conditions there are large additional losses. In reports of tests at supersonic speeds[1,2] these additional losses have been ascribed to the turning of the flow in the duct downstream of the cowl lip. In Fig.12 the losses in the present case are plotted against ω, the angle of turning between the front and rear movable ramps. The correlation is again quite good, although the loss at δ_2 equal to 9^o seems to be rather high. Some explanation of this may be contained in Fig.14. This shows the pressure distribution on the vertical centre line of the duct obtained from a pitot rake near the rear hinge position as shown in Fig.3. For each value of δ_2 and bleed exit area the pressure distribution is shown for successive points on the pressure recovery-mass flow characteristic, progressing from a supercritical condition, through critical, to a subcritical condition. At values of δ_2 of 5^o and above, where the minimum duct area is in the region of the bleed slot, the pressure distributions indicate that at supercritical flow conditions the flow at the pitot rake is supersonic. Fig.13 shows a comparison of the pressure recovery indicated by the pitot tubes in the middle of the duct when the intake is just supercritical, with the pressure recovery calculated from the assumption that the Mach number at the rake is derived from the area ratio A_t/A_R and $M_t = 1.0$.

The correspondence is quite good. This expansion over the rear ramp will inevitably be followed by a normal shock system which in general will be practically extinguished at the critical point. Most of the additional losses will be associated with separation occurring on the surface of the rear ramp. However, at the relatively high δ_2 of 9^o, followed by a rapidly expanding duct downstream of the throat, there is probably still some significant shock loss at the critical flow condition.

5.2 Intake mounted on a fuselage with compression surfaces horizontal

Pressure recovery-mass flow characteristics for the intake when installed on the fuselage with its leading edge horizontal are shown in Fig.15. The data were obtained at a constant bleed unit area (A_B/A_e) equal to 0.10 and for values of second ramp angle δ_2 equal to -10^o, 0^o and 5^o. As was the case with the isolated intake varying the angle of incidence had no effect on these characteristics within the range investigated.

In Figs.16a and 16b maximum total mass flow and maximum engine face mass flow are shown plotted against second wedge angle δ_2 for the intake alone and for the intake on the fuselage. Estimates of mass flow based on intake internal geometry have been calculated and are included for comparison. The presence of the fuselage causes a reduction in maximum total mass flow of about 1.5 per cent.

The difference in approach Mach number between the isolated intake and the intake on the fuselage is not known; all mass flows have been referred to nominal free stream Mach number. However, the difference is hardly likely to be the cause of this reduction in total flow because there is no corresponding reduction in engine face mass face. The deficit is entirely in the bleed flow quantity and is more probably caused by a change in bleed exit conditions due to the presence of the fuselage.

Measured maximum engine face mass flow falls below the quantity estimated from the intake internal geometry because of the apparent throat size referred to in section 5.1. The difference between the measured maximum total mass flow and the estimate based on the inlet area at the cowl lip has one of two origins depending on the particular value of δ_2. For values of δ_2 above about 2^o it is due largely to choking at the bleed inlet and consequent failure of the bleed to operate. At lower values of δ_2 it is due simply to insufficient bleed exit area.

The negligible effect of the fuselage flow field on intake pressure recovery is illustrated in Figs.16c and 16d which show the variation with δ_2

of both critical point and maximum pressure recovery for the isolated intake and the intake on the fuselage. Estimates of skin friction and interference losses based on Ref.6 are also shown on this figure to illustrate the large additional pressure recovery losses referred to in section 5.1.

5.3 Intake mounted on the fuselage with compression surfaces vertical

Figs.17 to 22 show pressure recovery-mass flow characteristics for the intake when mounted on the fuselage with its leading edge vertical. The intake was fitted with either two swept endwalls or two unswept endwalls. Details of the endwall shapes are shown in Fig.4. For each endwall configuration data are presented for a constant second ramp angle equal to -10°, with bleed exit areas (A_B/A_e) of 0.05, 0.10 and 0.174, and a range of incidence of the intake-fuselage assembly from zero to 12°.

In Fig.23 the variation of mass flow and pressure recovery with bleed exit area is summarised for both endwall configurations. Removing the swept endwalls reduces the large loss in maximum pressure recovery which occurs at an incidence of 12°.

5.4 Comparison between vertical intake and horizontal intake

The mass flows and pressure recoveries of the various configurations of the intake when mounted on the fuselage are shown in Fig.24 for a second ramp angle of -10° and a bleed exit area (A_B/A_e) equal to 0.10. The indications are that at low angles of incidence ($\alpha = 0^{\circ}$ to 4°) there is little difference between any of the configurations. However, the intake with its compression surfaces vertical is affected by incidences above 4°. In particular the configuration with two swept endwalls suffers a significant loss in maximum pressure recovery at an incidence of 12°.

5.5 Engine face distortion

Distortion at the engine face expressed as DC_{60} is shown in Fig.25. The maximum subcritical value of DC_{60} is also shown. This is rarely greater than the value at the critical point and in any case always occurs within 5 per cent of maximum mass flow. At low angles of incidence, up to about 4°, the value of DC_{60} is in the region -0.25 to -0.35 for all configurations. However, at angles of incidence beyond 4° the intake with the vertical leading edge shows some deterioration in flow uniformity whereas with the leading edge horizontal the uniformity is apparently unaffected.

6 CONCLUSIONS

Measurements have been made of the internal performance of a rectangular intake having variable geometry and designed for supersonic operation. The measurements were made at a Mach number of 0.9 and a Reynolds number based on intake entry height of approximately 10^6. The intake has been tested through a range of angle of incidence of 0^o to 10^o in isolation in a uniform flow field and in the environment generated by a particular shape of fuselage.

Maximum mass flow is slightly less than would be estimated on the basis of geometric throat size; the deficit corresponds to a reduction in throat size of about 3 per cent.

Internal contraction, where it is located in the region of the bleed slot, leads to a failure of bleed operation at maximum mass flow.

Critical point pressure recovery is well below that predicted after taking into account duct losses. However, as was the case at supersonic speeds, these additional losses correlate well with the turning angle between the front and rear movable ramps.

With the compression surfaces of the intake horizontal there was no deterioration in performance with increase in angle of incidence; nor was the performance impaired by the presence of this particular fuselage.

With compression surfaces vertical, the intake on the fuselage, suffered some loss in mass flow and pressure recovery at angles of incidence above 4^o This was only partly alleviated by removing the swept endwalls.

NOTATION

A_B	bleed exit area
A_D	bleed duct cross-sectional area
A_R	cross-sectional area at the rake station near the rear hinge
A_f	engine face cross-sectional area
A_X	cross-sectional area at station X
K	discharge coefficient
L	distance from the cowl lip to the rear hinge
M	Mach number
P	total pressure
P_R	pitot pressure at the rake station near the rear hinge
q	dynamic pressure
p	static pressure
X	distance downstream of cowl lip
α	angle of incidence of intake relative to free stream
δ_1	angle between first compression surface and free stream ahead of intake
δ_2	angle between first and second compression surfaces
ω	angle between front and rear movable ramps

Subscripts

C	at critical flow conditions
B	in the bleed
e	in the intake entry plane
f	at the engine face
i	at the cowl lip
t	at the section of duct minimum area
T	total, i.e. engine plus bleed
X	at station X
∞	in the free stream

REFERENCES

No.	Author	Title, etc.
1	C.S. Brown E.L. Goldsmith	Measurement of the internal performance of a rectangular air intake with variable geometry. Part I. ARC CP No.1243 (1971)
2	C.S. Brown E.L. Goldsmith	Idem. Part II. The effect of incidence. ARC CP No.1292 (1971)
3	C.S. Brown E.L. Goldsmith	Measurement of the internal performance of a rectangular air intake mounted on a fuselage at Mach numbers from 1.6 to 2. ARC CP No.1291 (1972)
4	E.L. Goldsmith	Variable geometry intakes at supersonic speeds. Some techniques and some test results. AGARD CP 34 (1968)
5	I. McGregor	The characteristics and calibration of two types of airflow metering device for investigating the performance of model air intakes. RAE Technical Report 71212 (ARC 33894) (1971)
6	J. Seddon	Boundary layer interaction effects in intakes with particular reference to those designed for dual subsonic and supersonic performance. ARC R & M 3565 (1966)

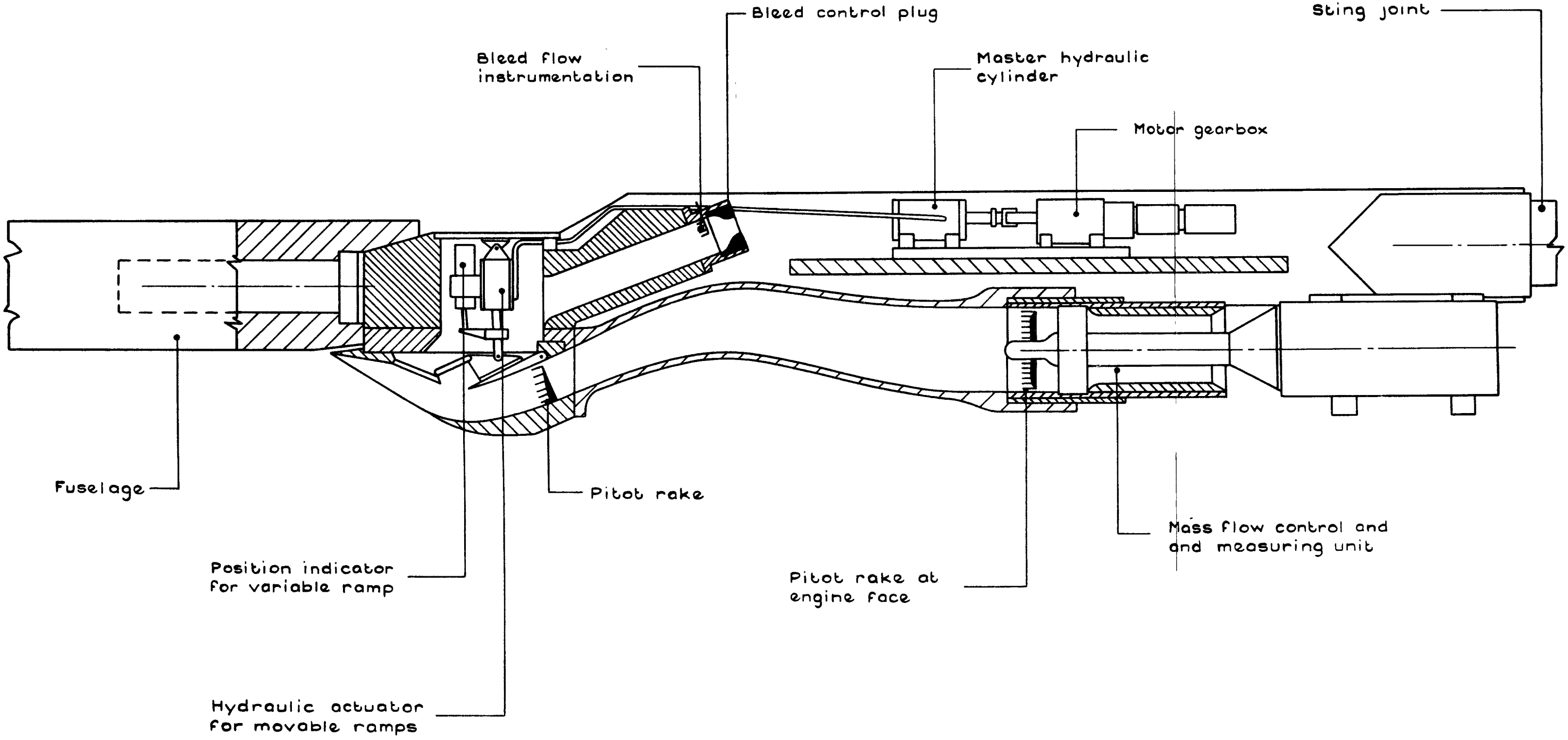

Fig. 1 General arrangement of intake and fuselage on test rig

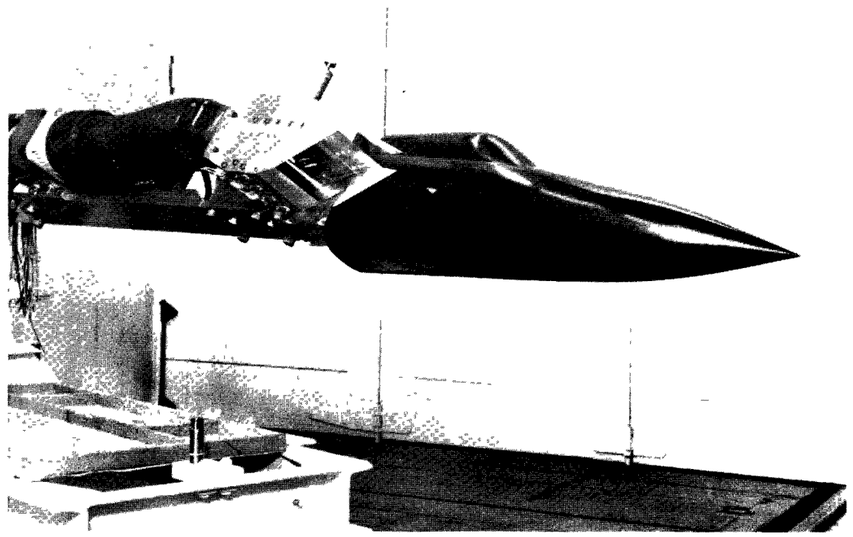

Fig.2a Fuselage and intake with compression surfaces horizontal assembled on intake test rig

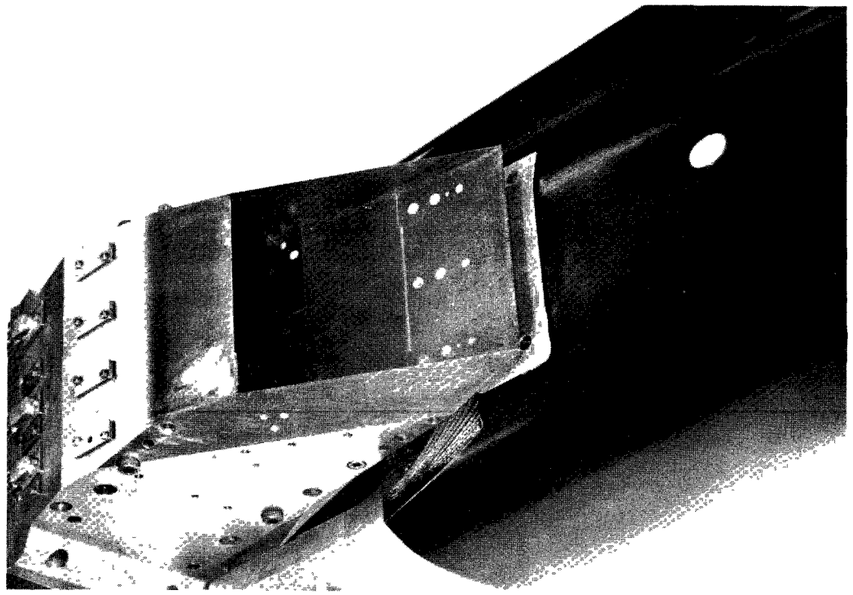

Fig.2b Intake with compression surfaces vertical assembled on fuselage

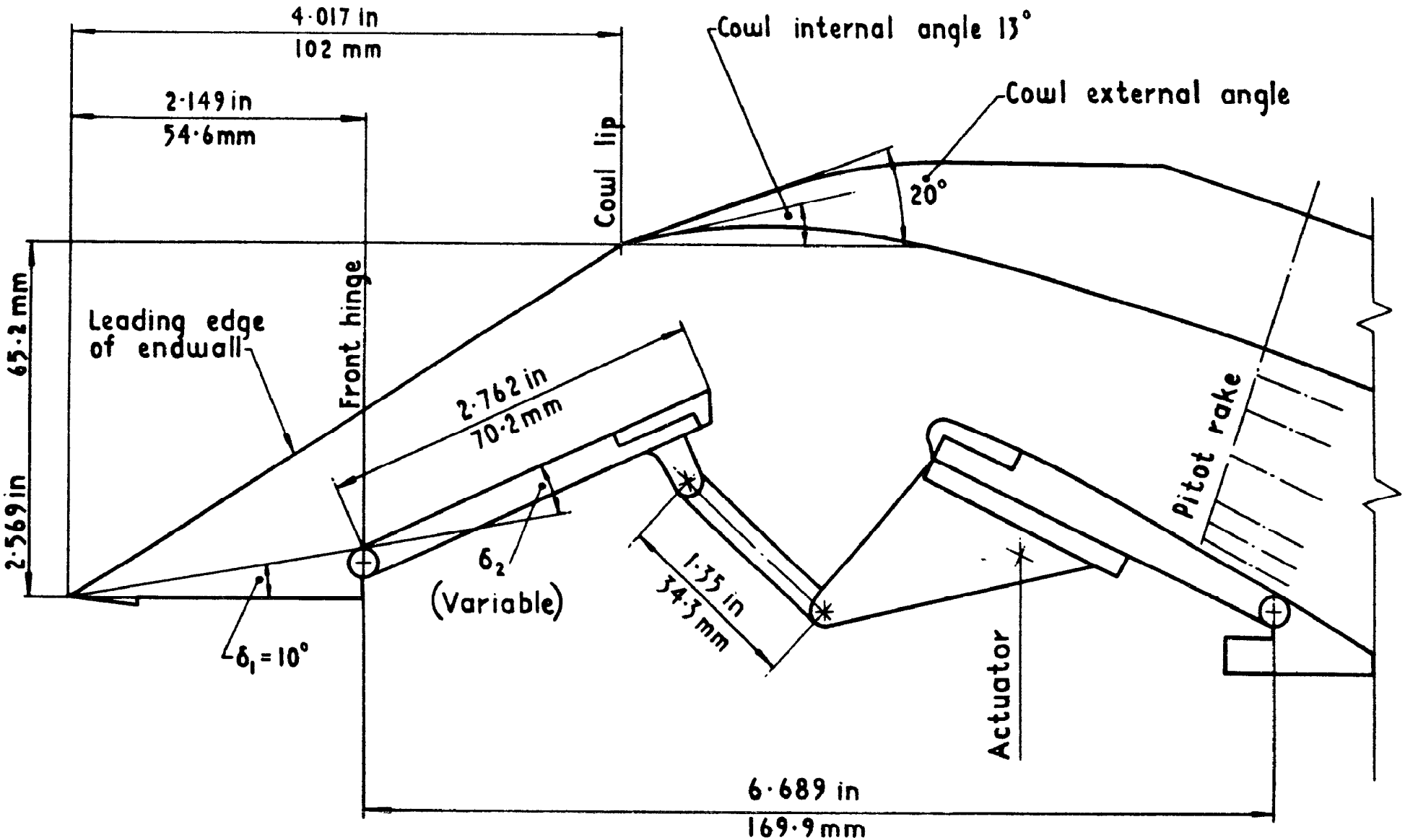

Fig.3 Geometry of compression surface ramps, cowl and bleed

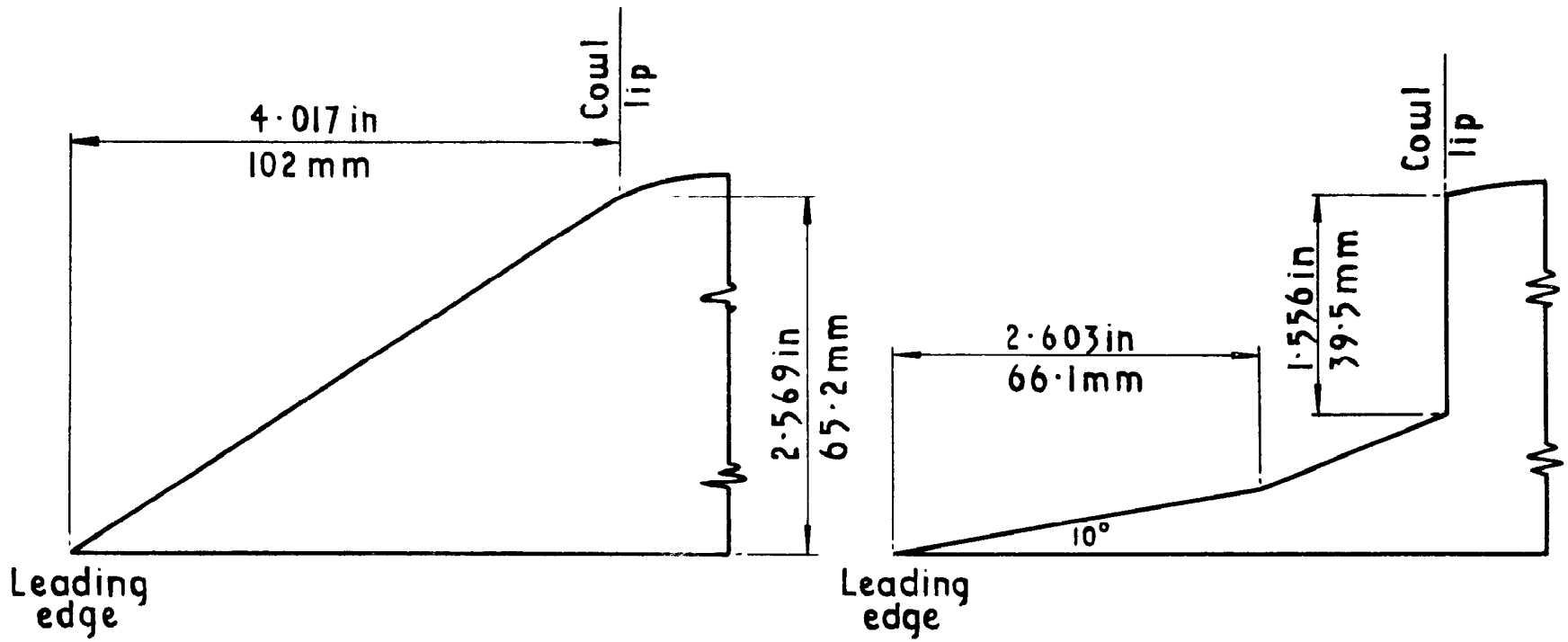

Fig.4 Details of endwalls

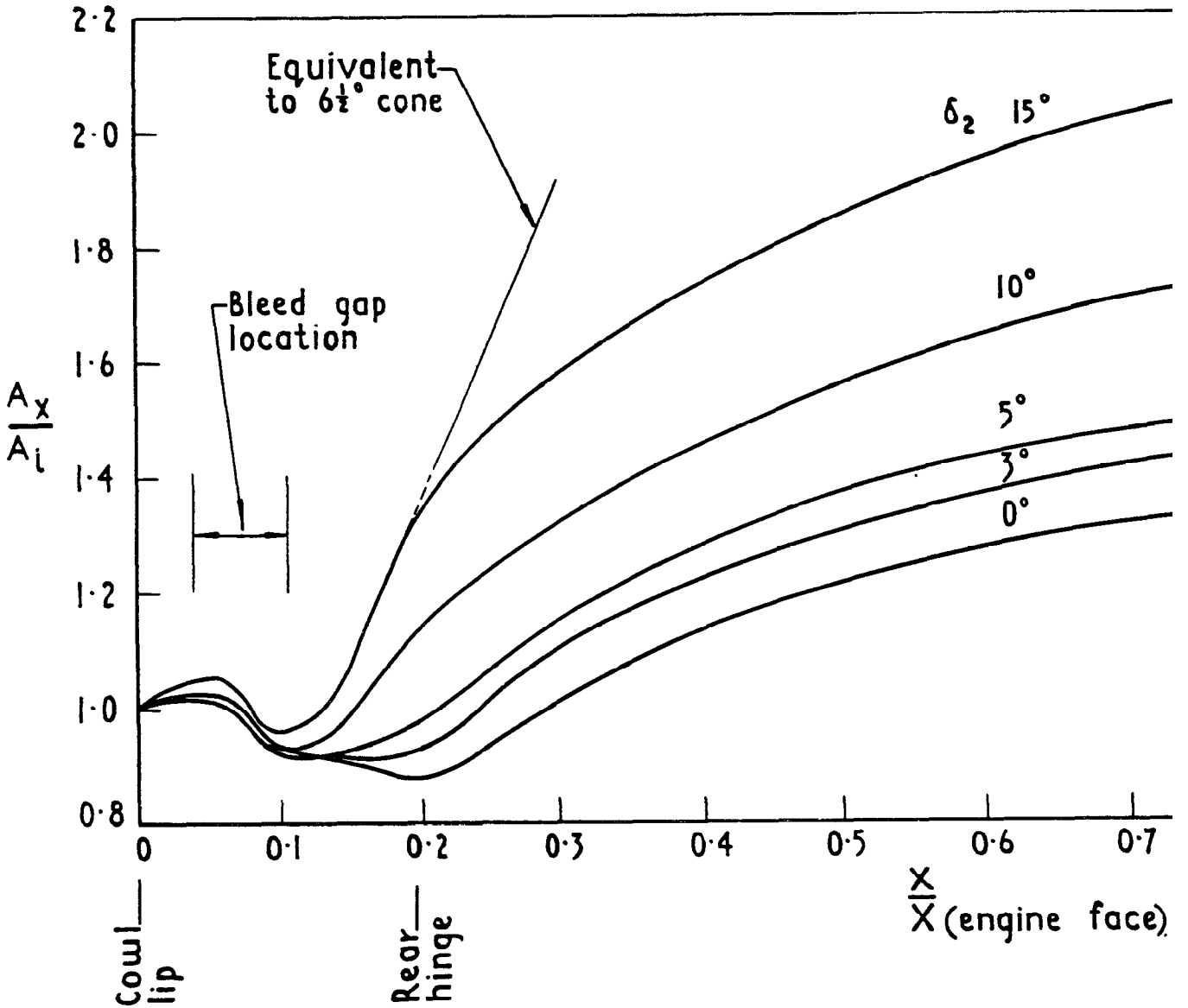

Fig.5a Area distribution through intake

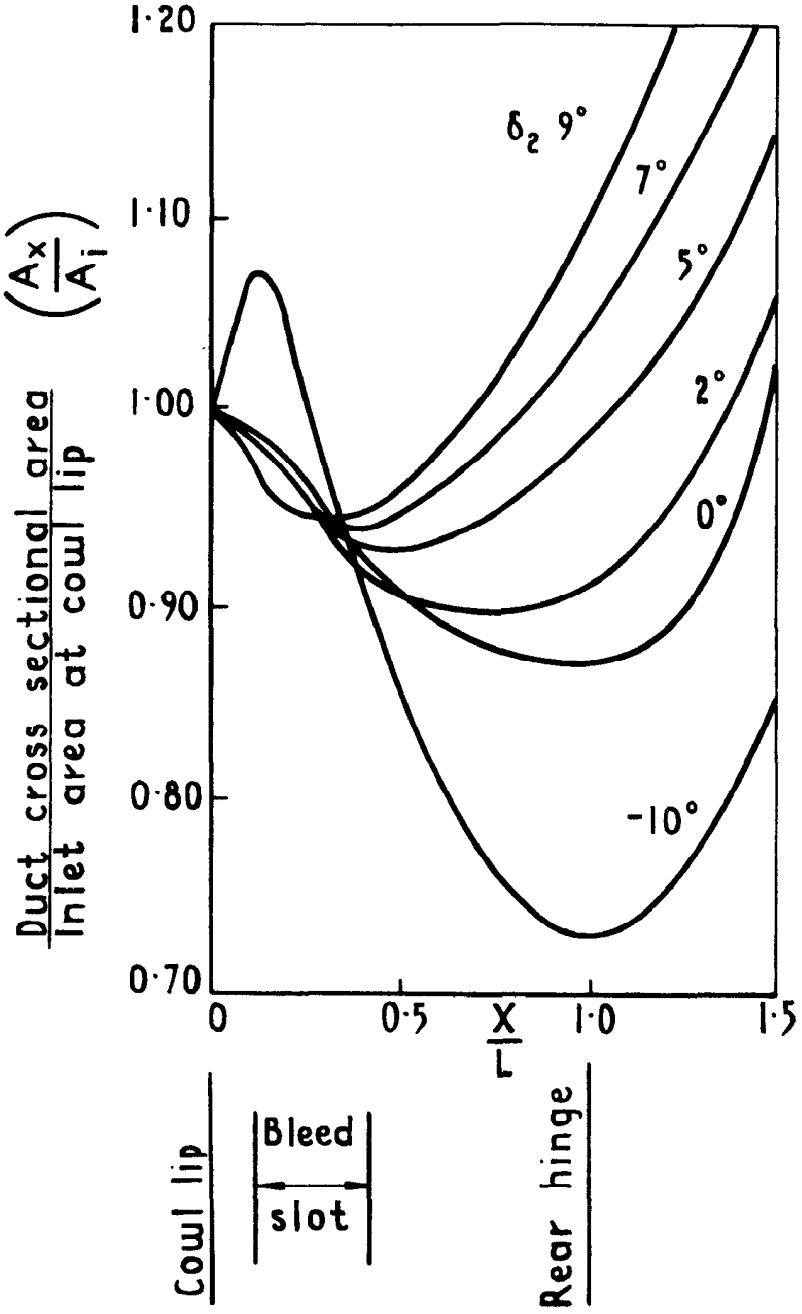

Fig. 5b Area distribution through intake between cowl lip and rear ramp hinge

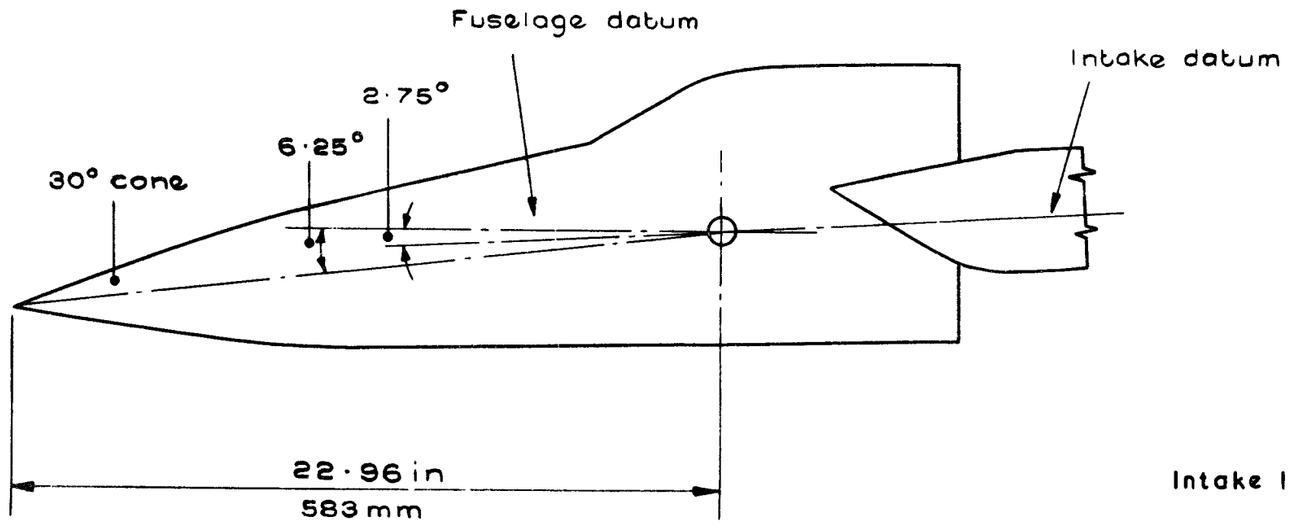

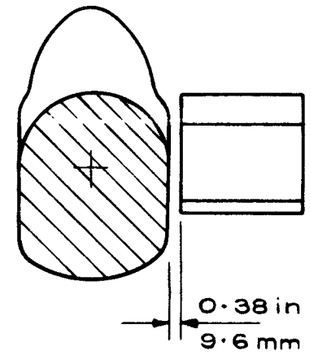

Intake leading edge horizontal

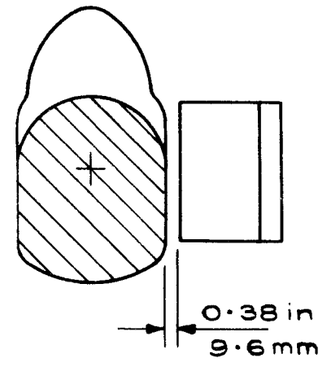

Intake leading edge vertical

Fig.6 Details of fuselage showing location of intake

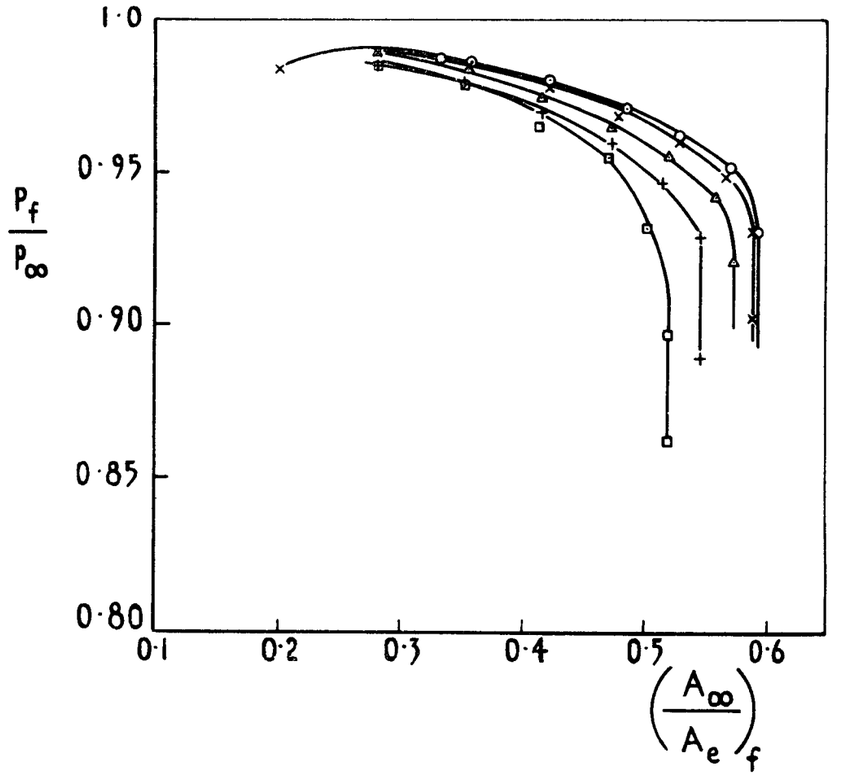

Fig.7 Variation of pressure recovery with mass flow. Isolated intake

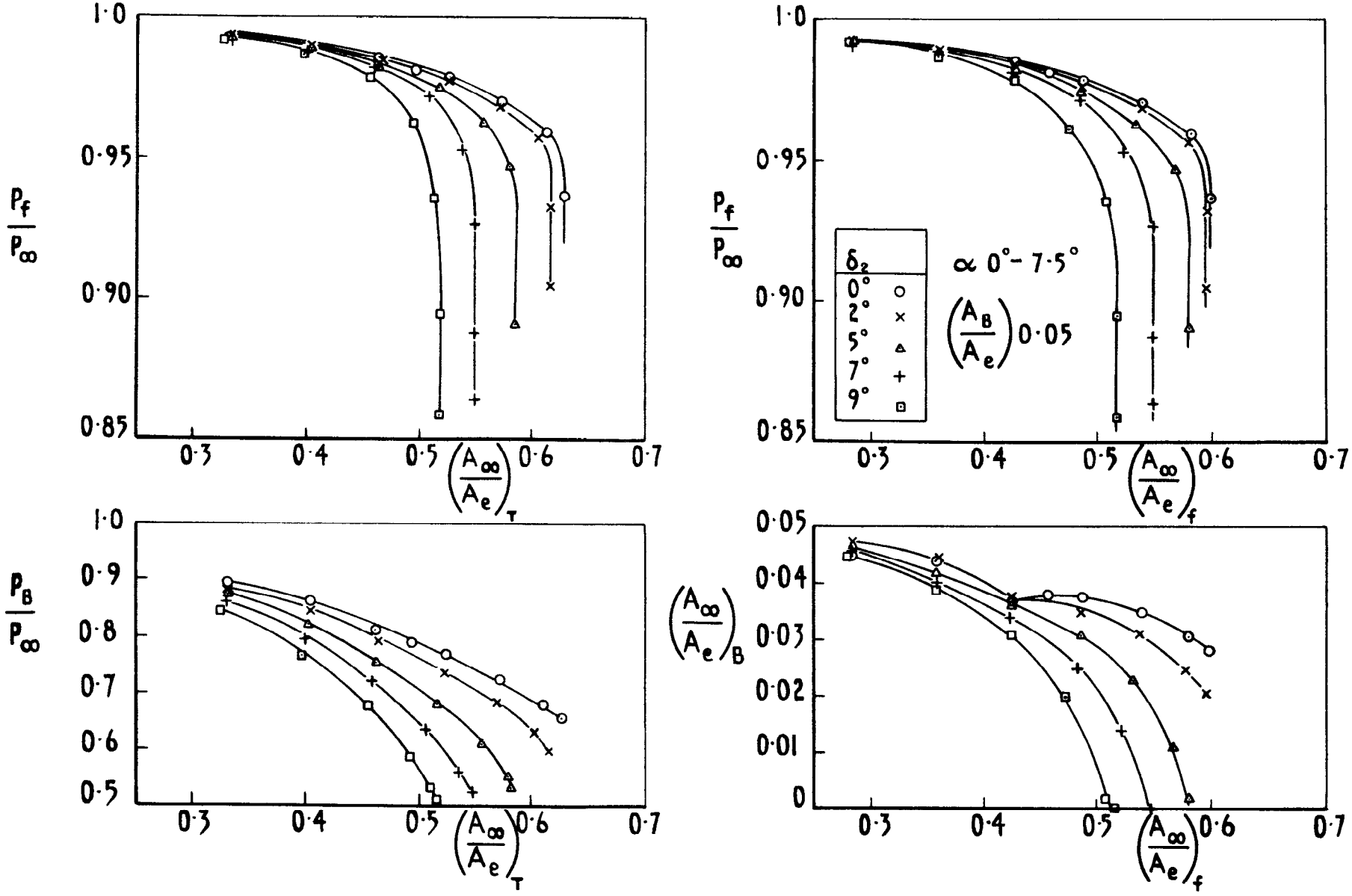

Fig.8 Variation of pressure recovery with mass flow.
Isolated intake

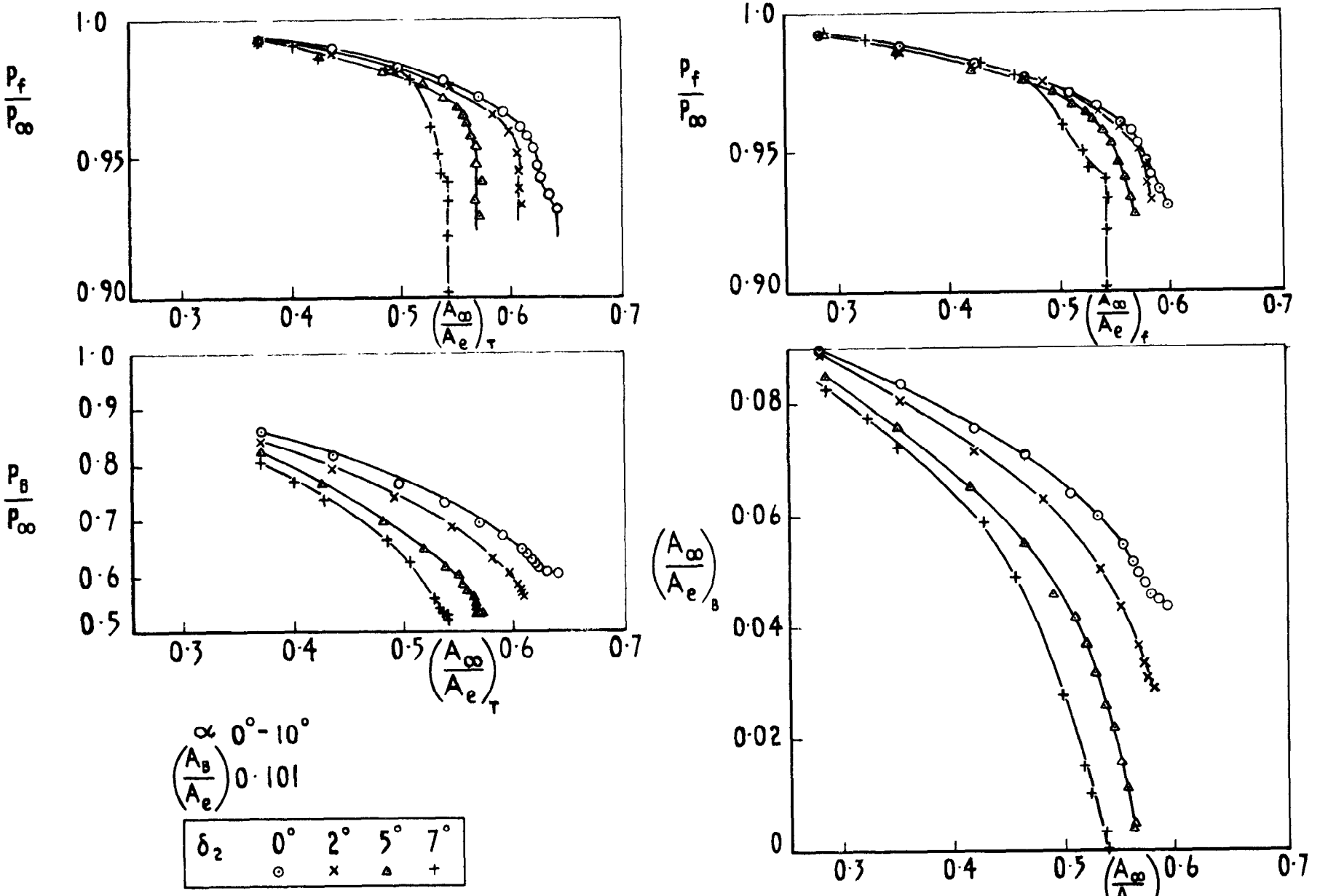

Fig.9 Variation of pressure recovery with mass flow. Isolated intake

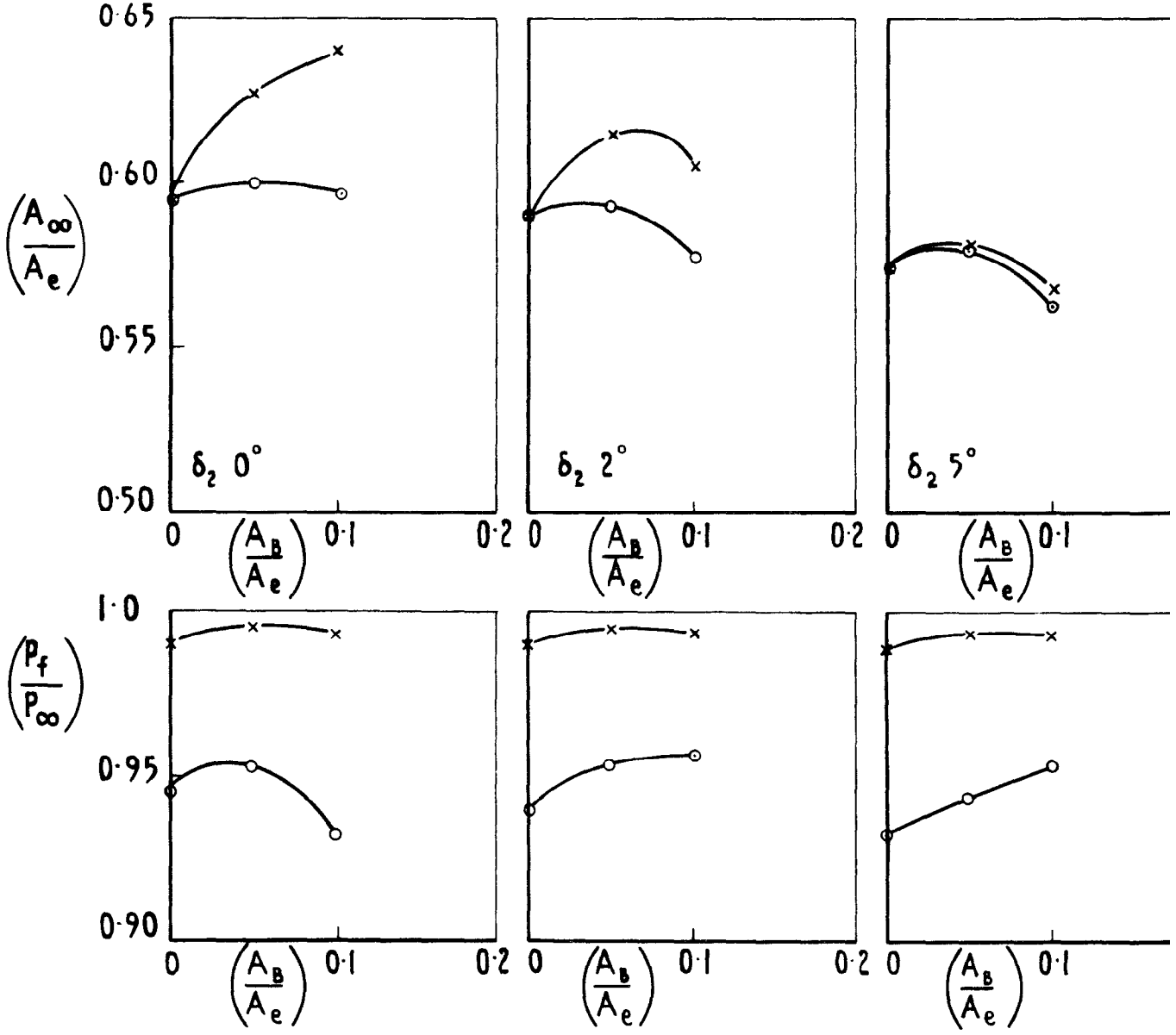

Fig.10 Variation of mass flow and pressure reco
bleed exit area. Intake alone. $\alpha = 0^\circ$

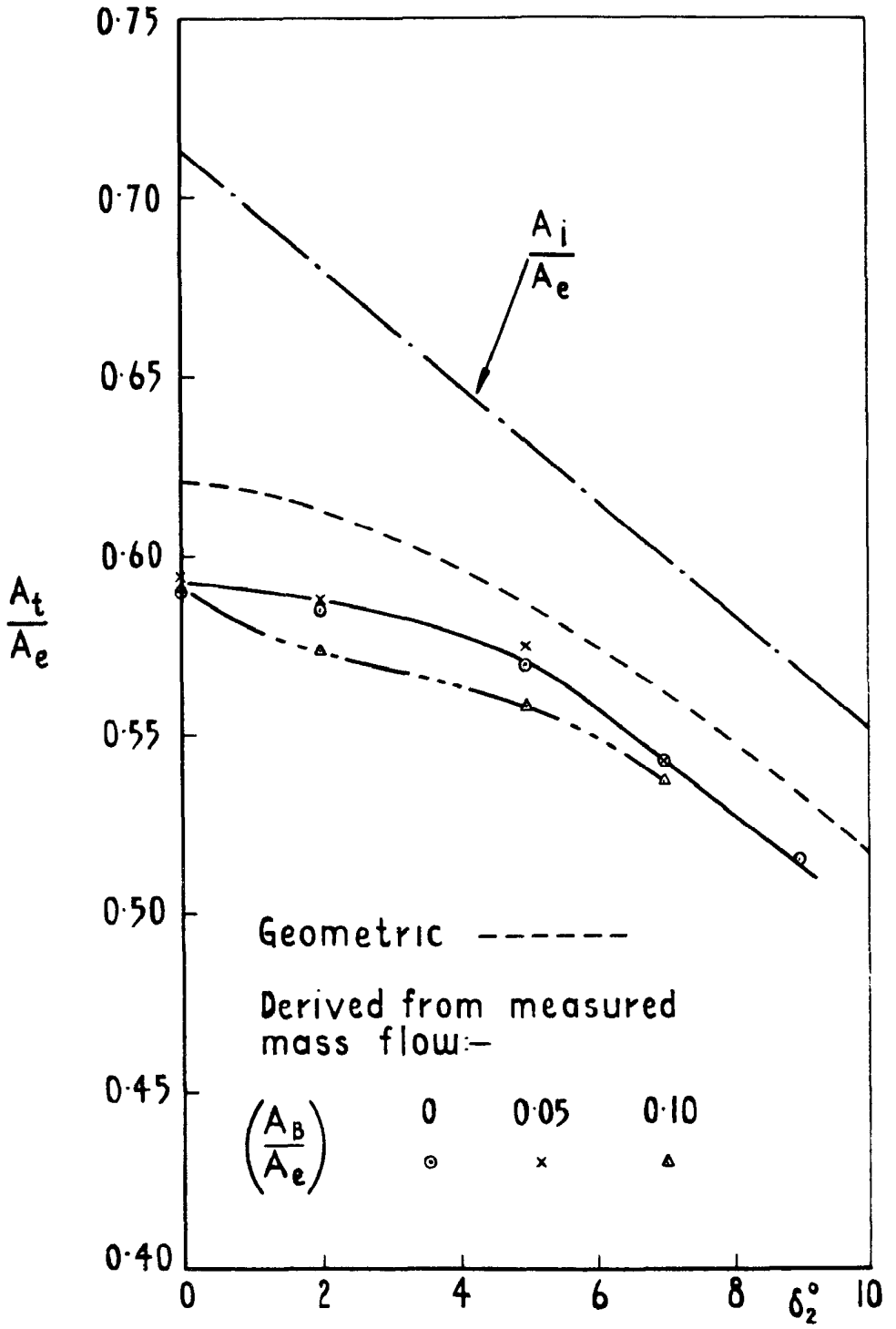

Fig. 11 Duct minimum area derived from measured mass flow. Isolated intake

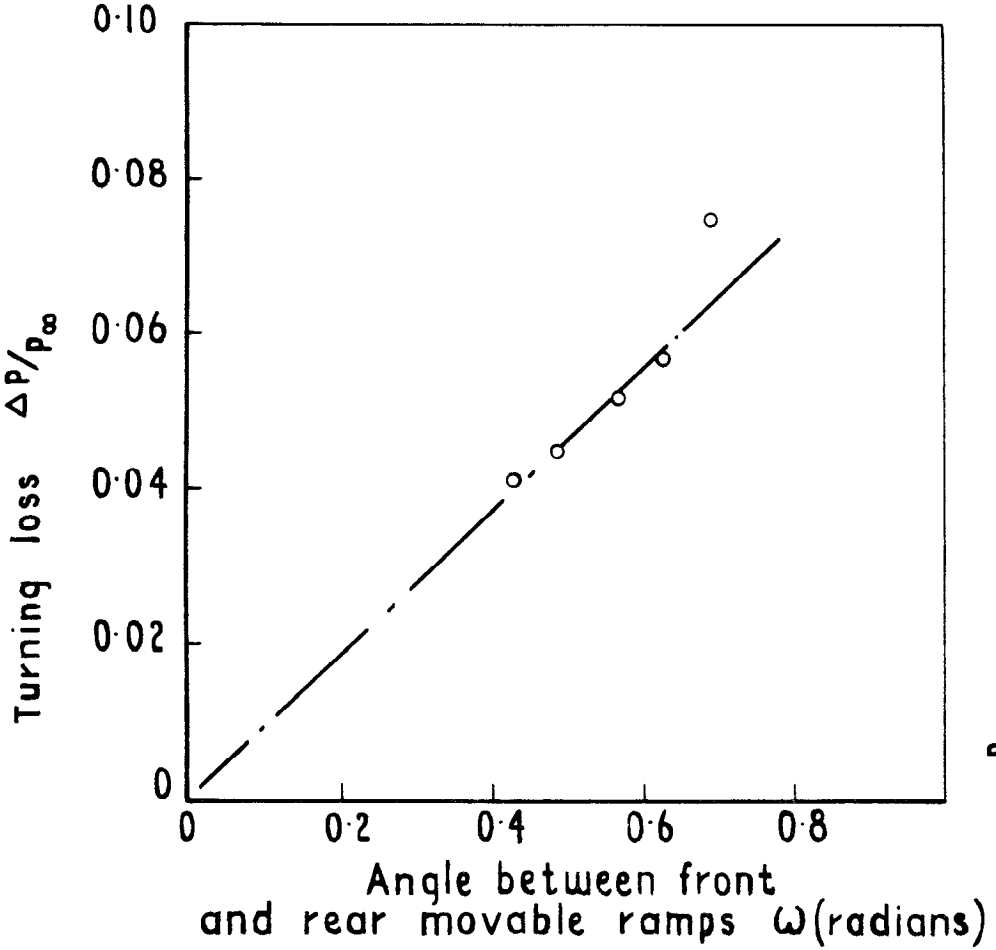

Fig.12 Correlation between flow turning loss and angle between front and rear movable ramps. Isolated intake. Zero bleed

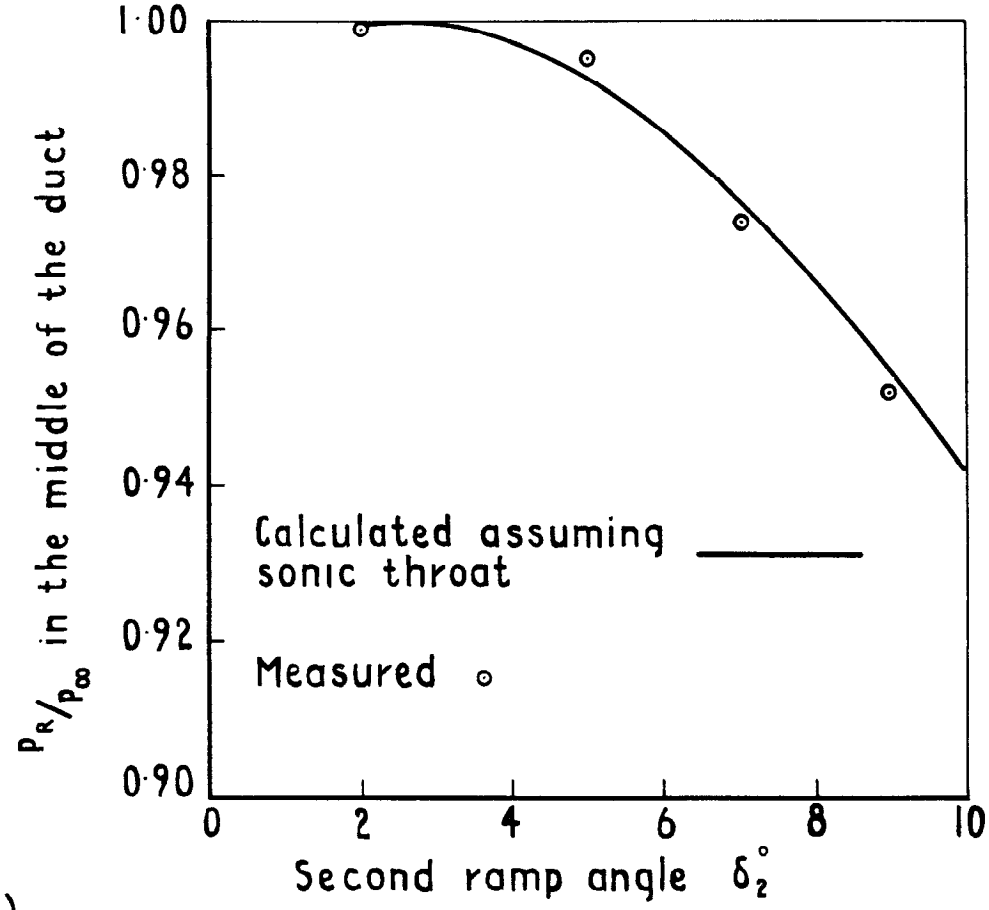

Fig.13 Pitot pressure at rear hinge position. Critical flow conditions. Isolated intake

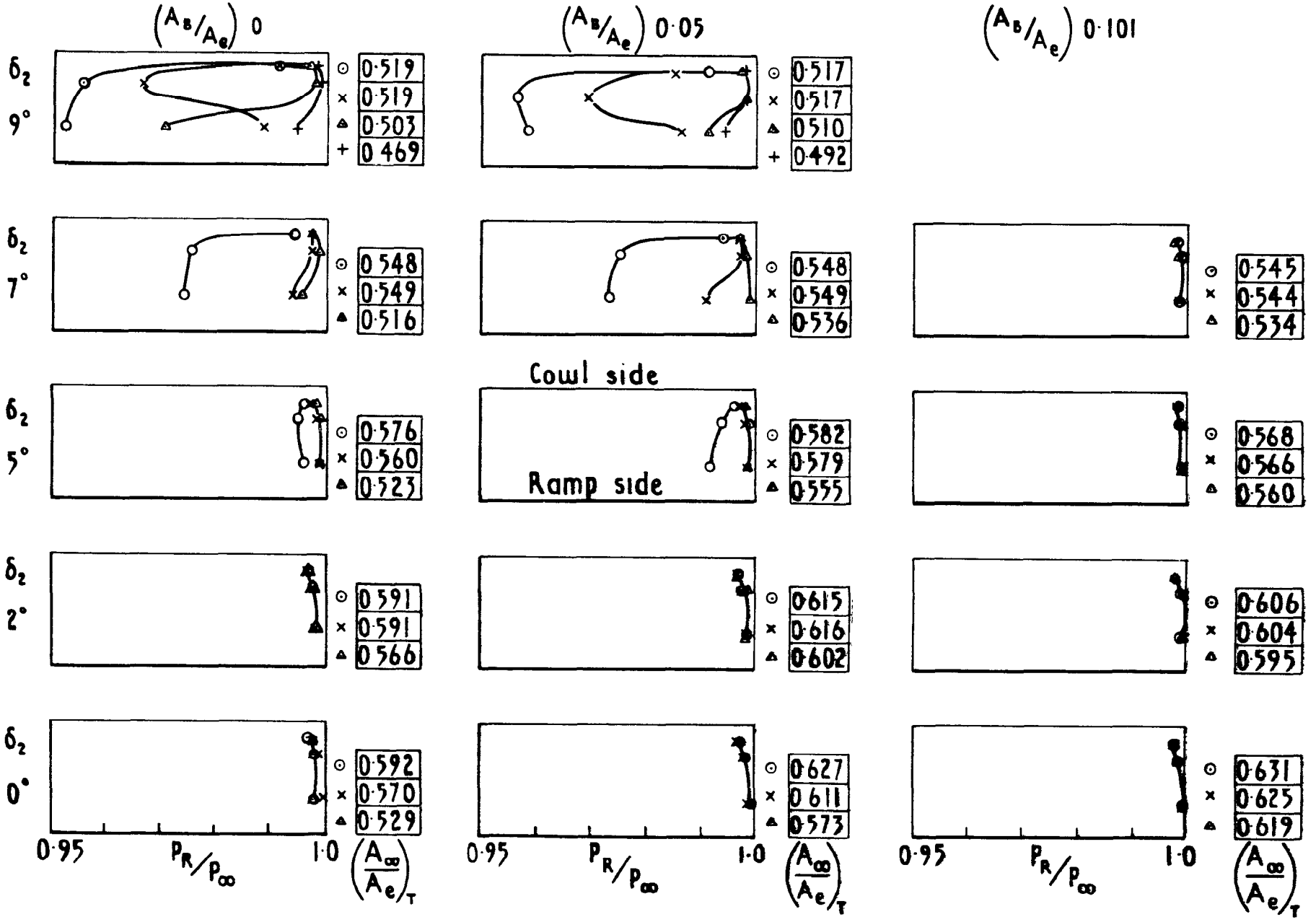

Fig. 14 Pressure distribution on duct vertical centre line at rear hinge position

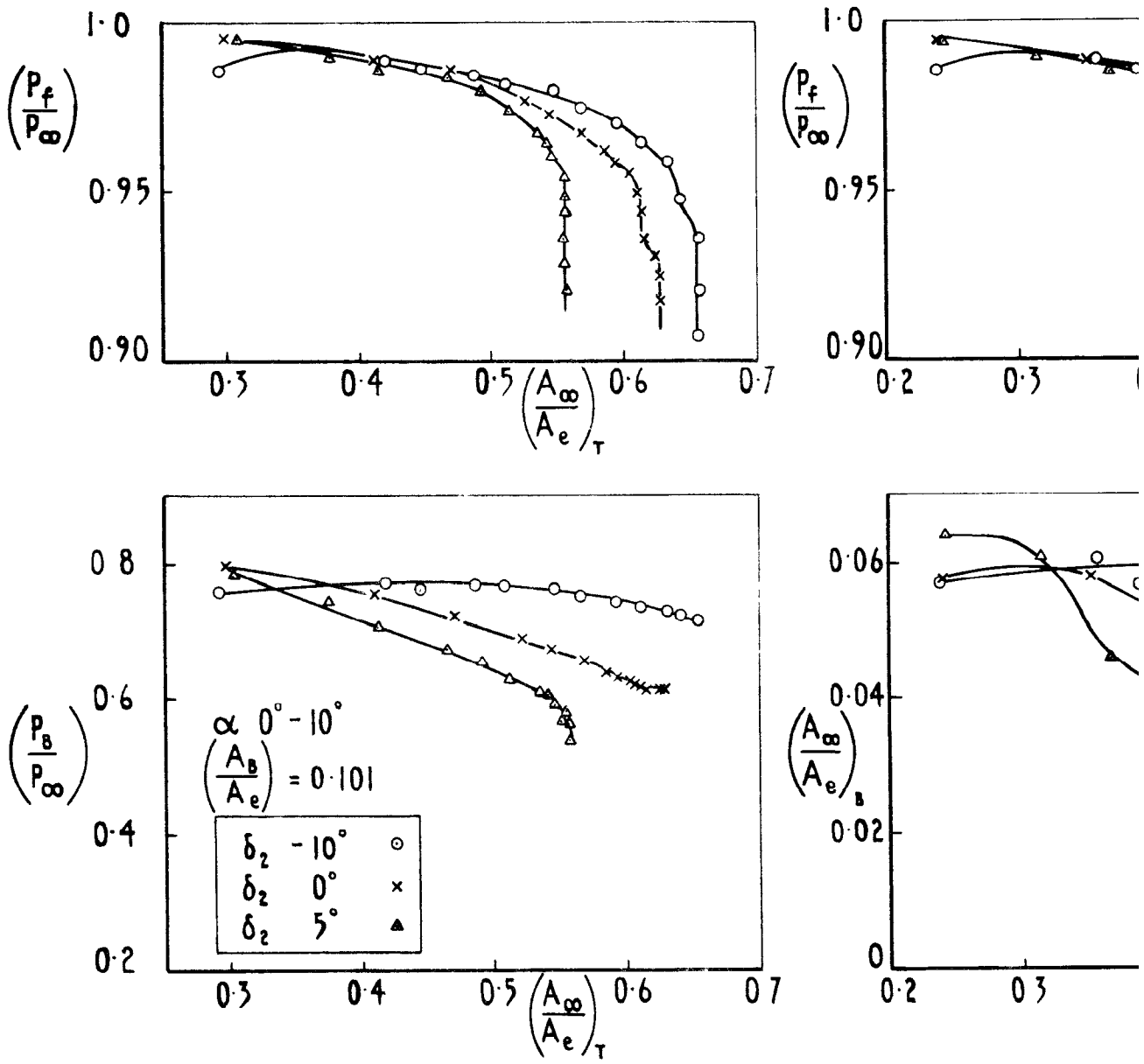

Fig.15 Variation of pressure recovery with r
Intake with swept endwalls on fuselage wit

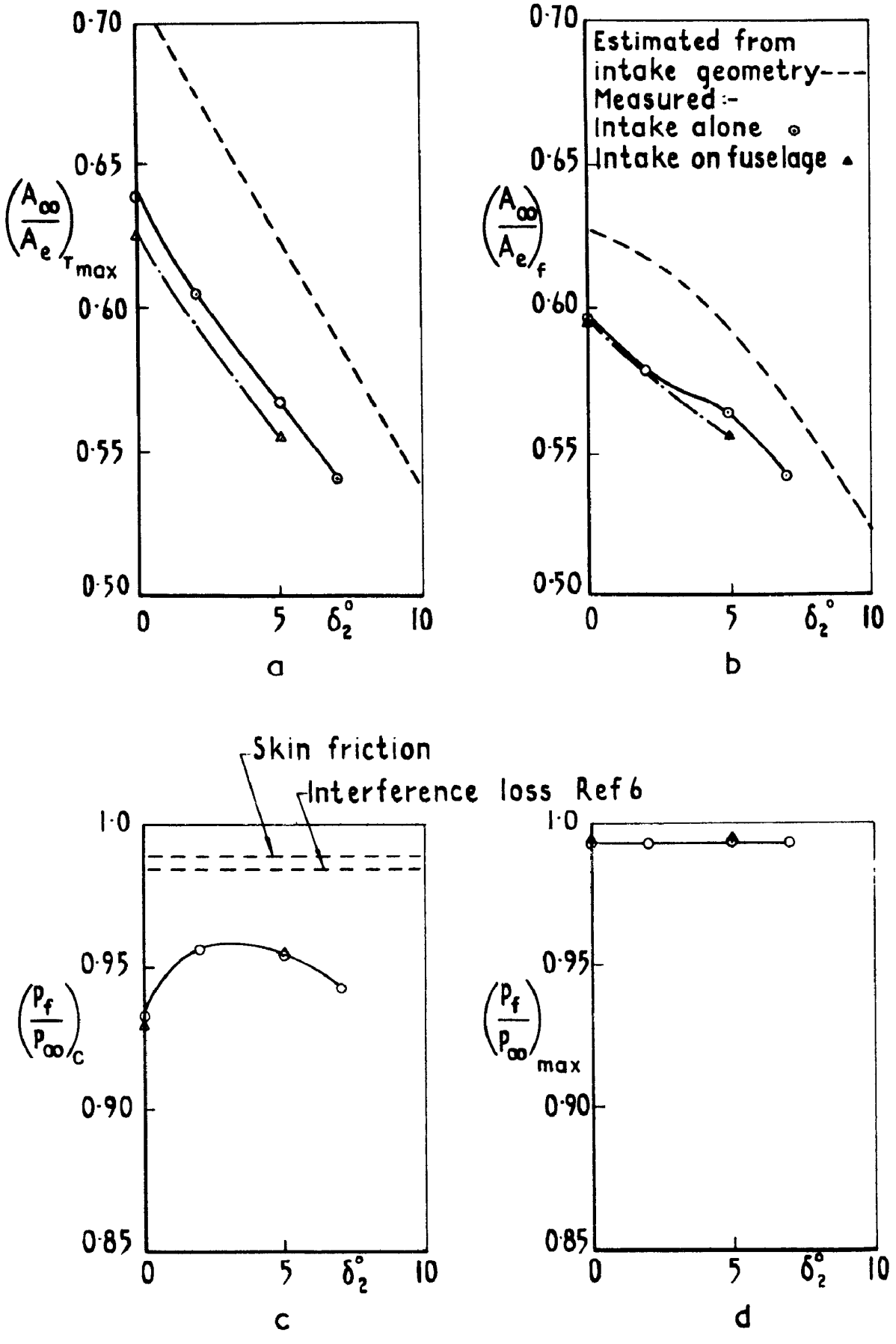

Fig. 16 a-d Variation of pressure recovery and maximum mass flow with δ_2. Intake alone & on fuselage with leading edge horizontal $\left(A_B/A_e\right) = 0 \cdot 101$

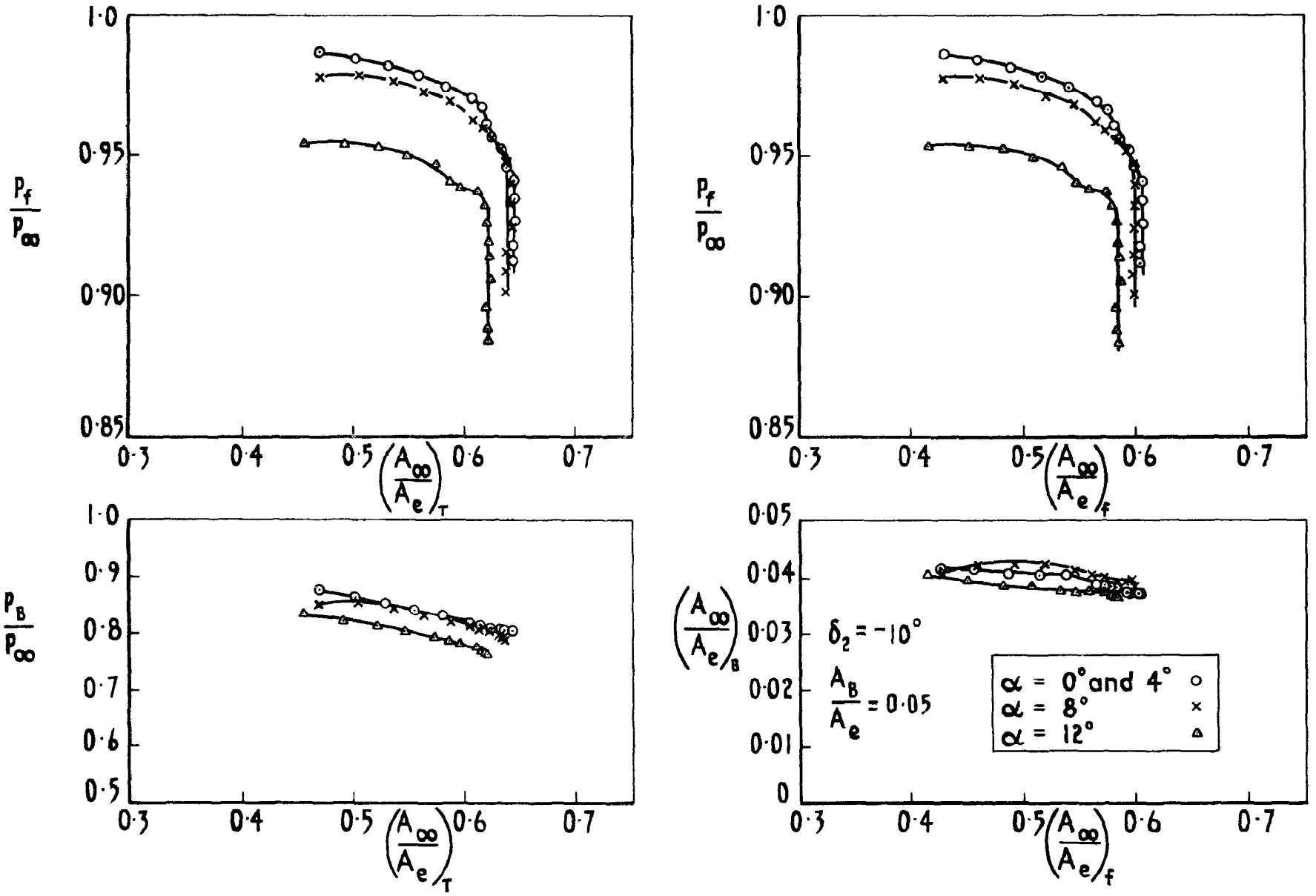

Fig.17 Variation of pressure recovery with mass flow. Intake with swept endwalls on fuselage with LE vertical

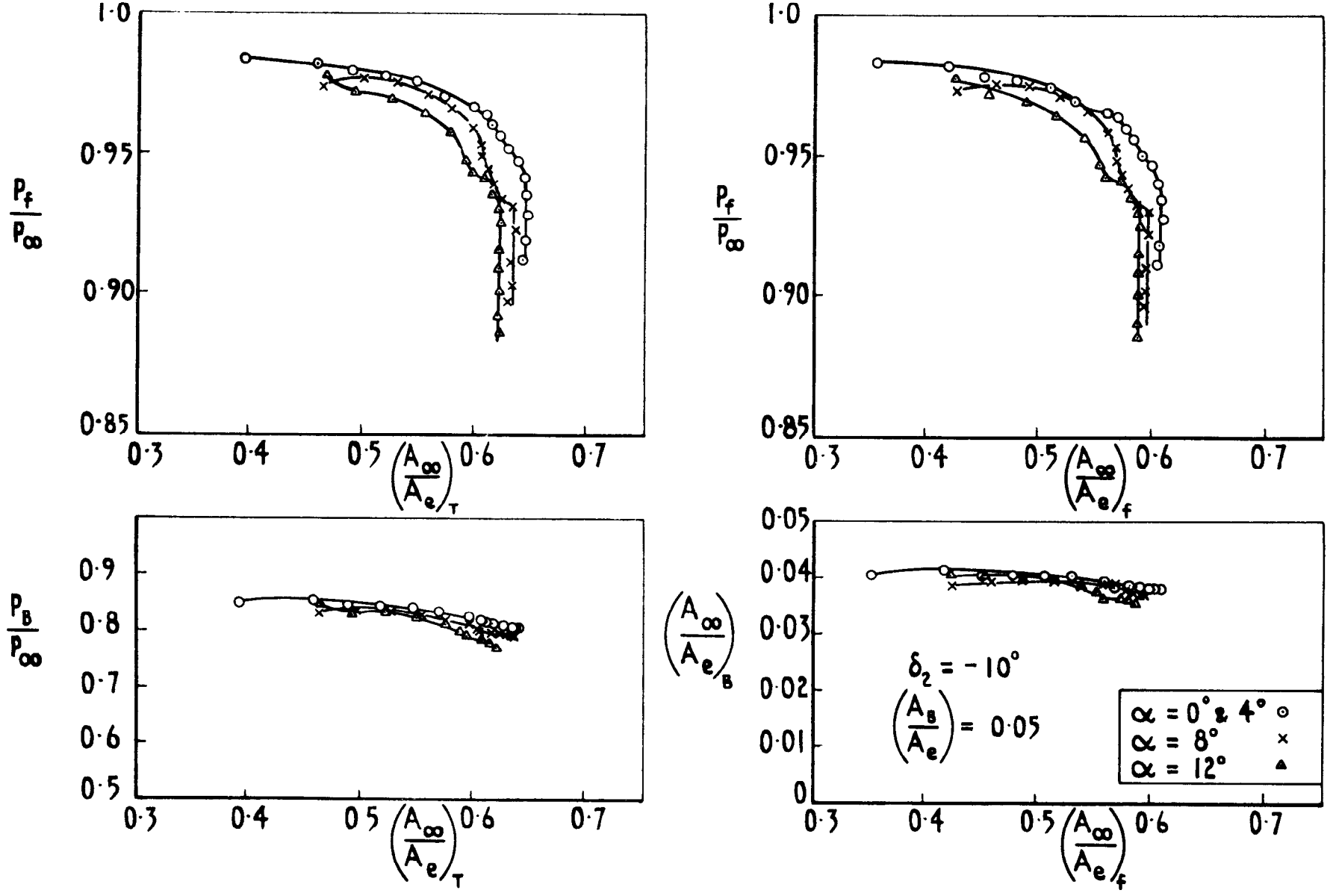

Fig. 18 Variation of pressure recovery with mass flow.
Intake with unswept endwalls on fuselage with L E vertical

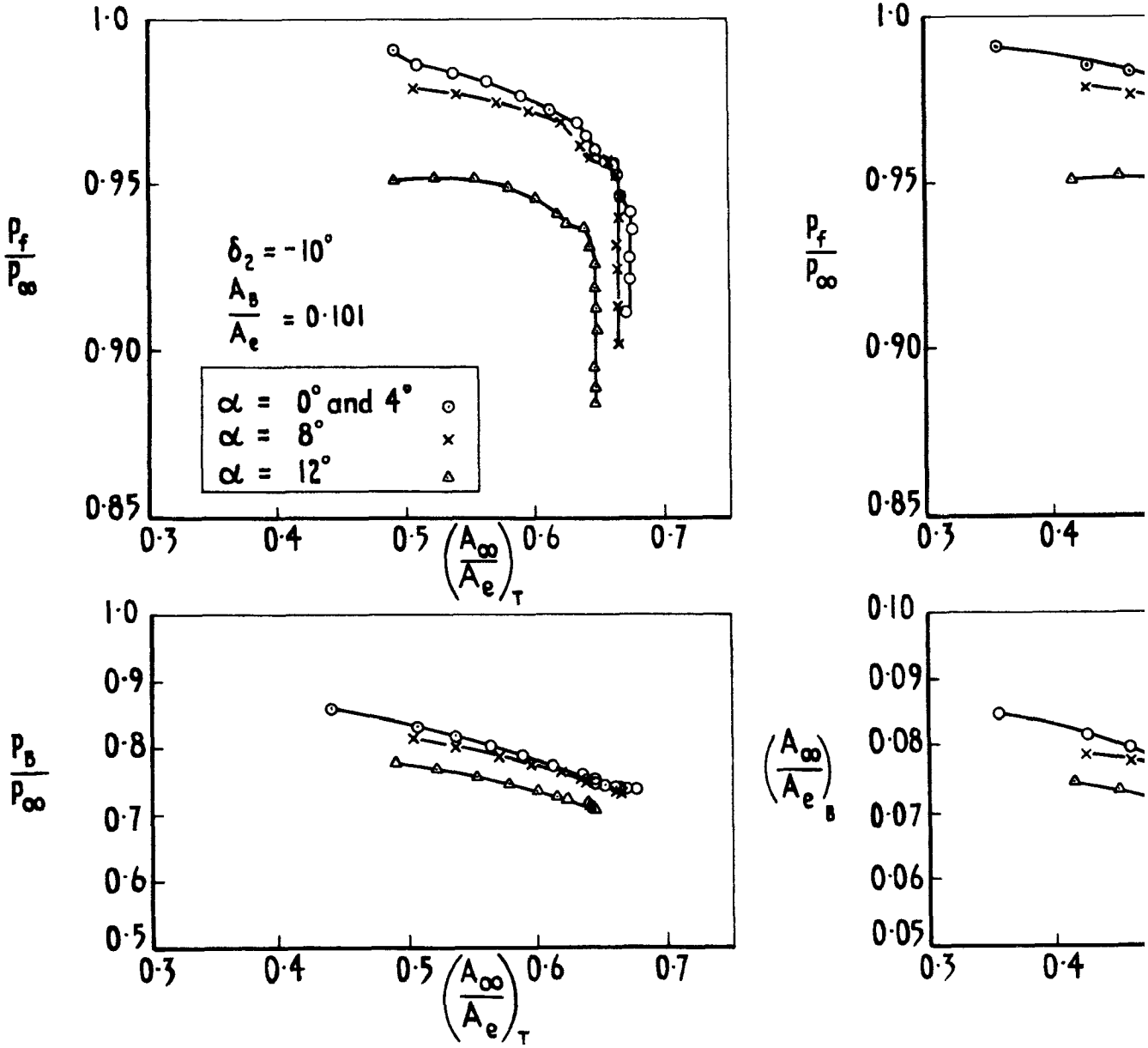

Fig.19 Variation of pressure recovery with Intake with swept endwalls on fuselage with

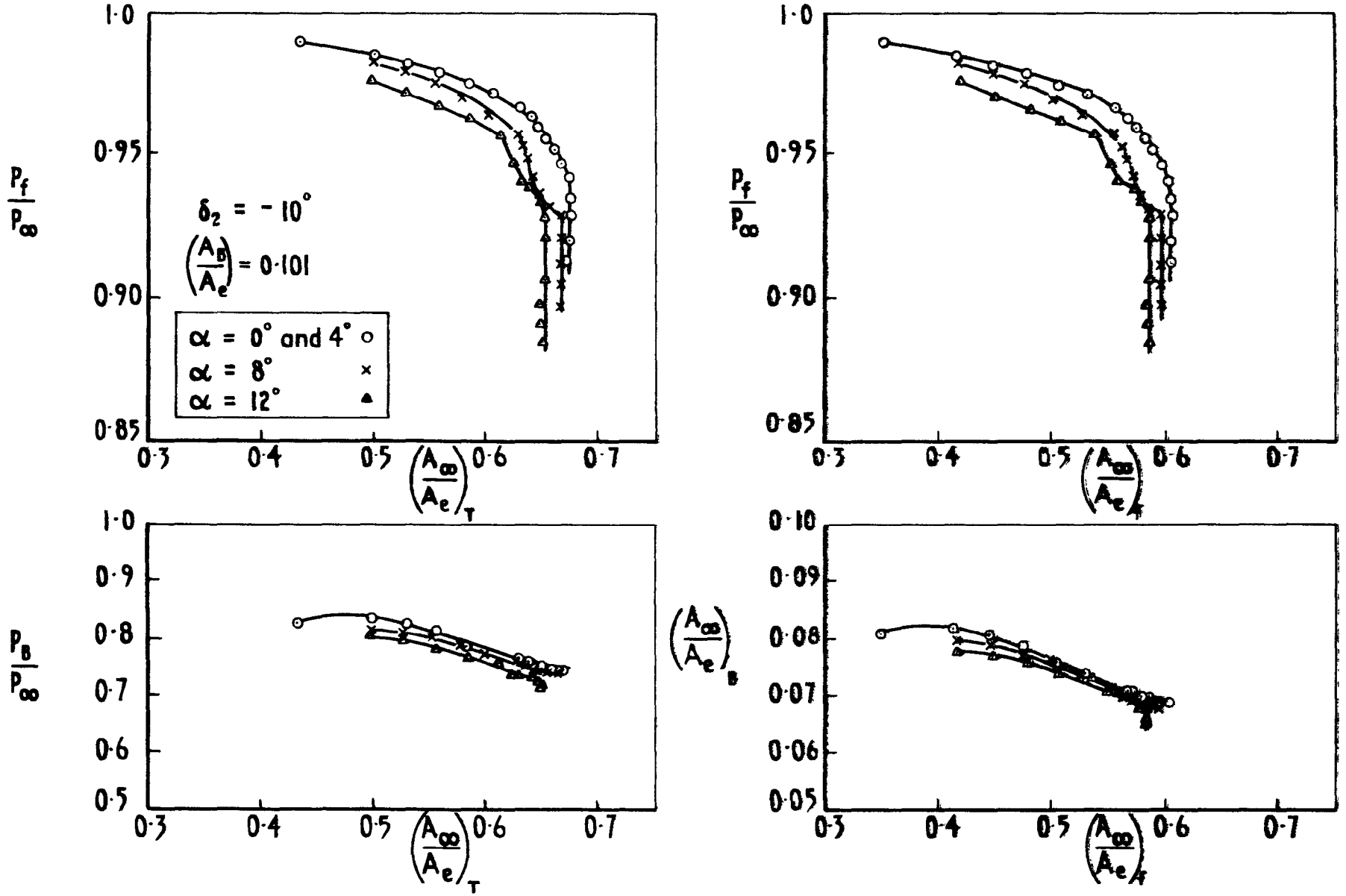

Fig. 20 Variation of pressure recovery with mass flow.
Intake with unswept endwalls on fuselage with L E vertical

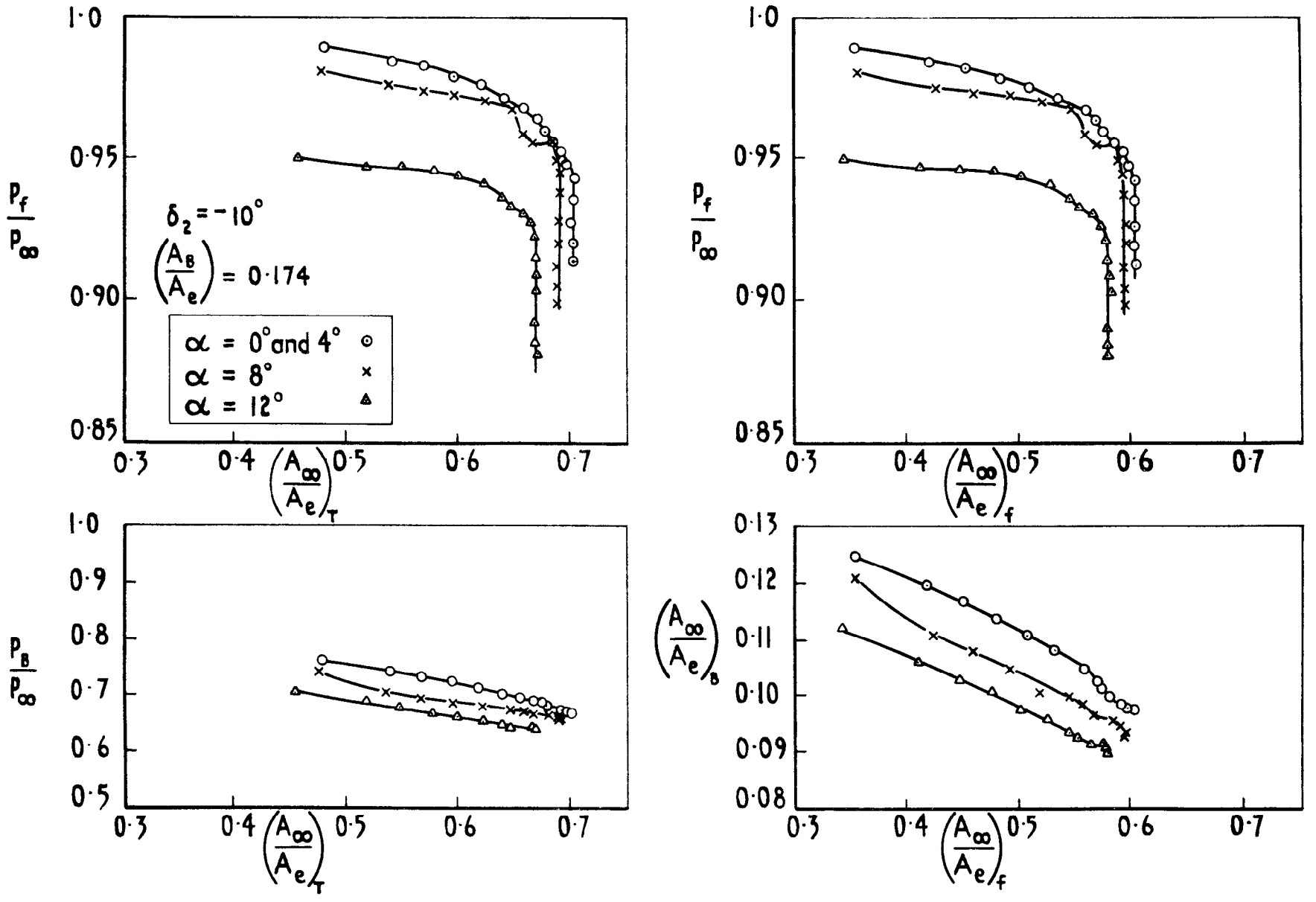

Fig.21 Variation of pressure recovery with mass flow. Intake with swept endwalls on fuselage with LE vertical

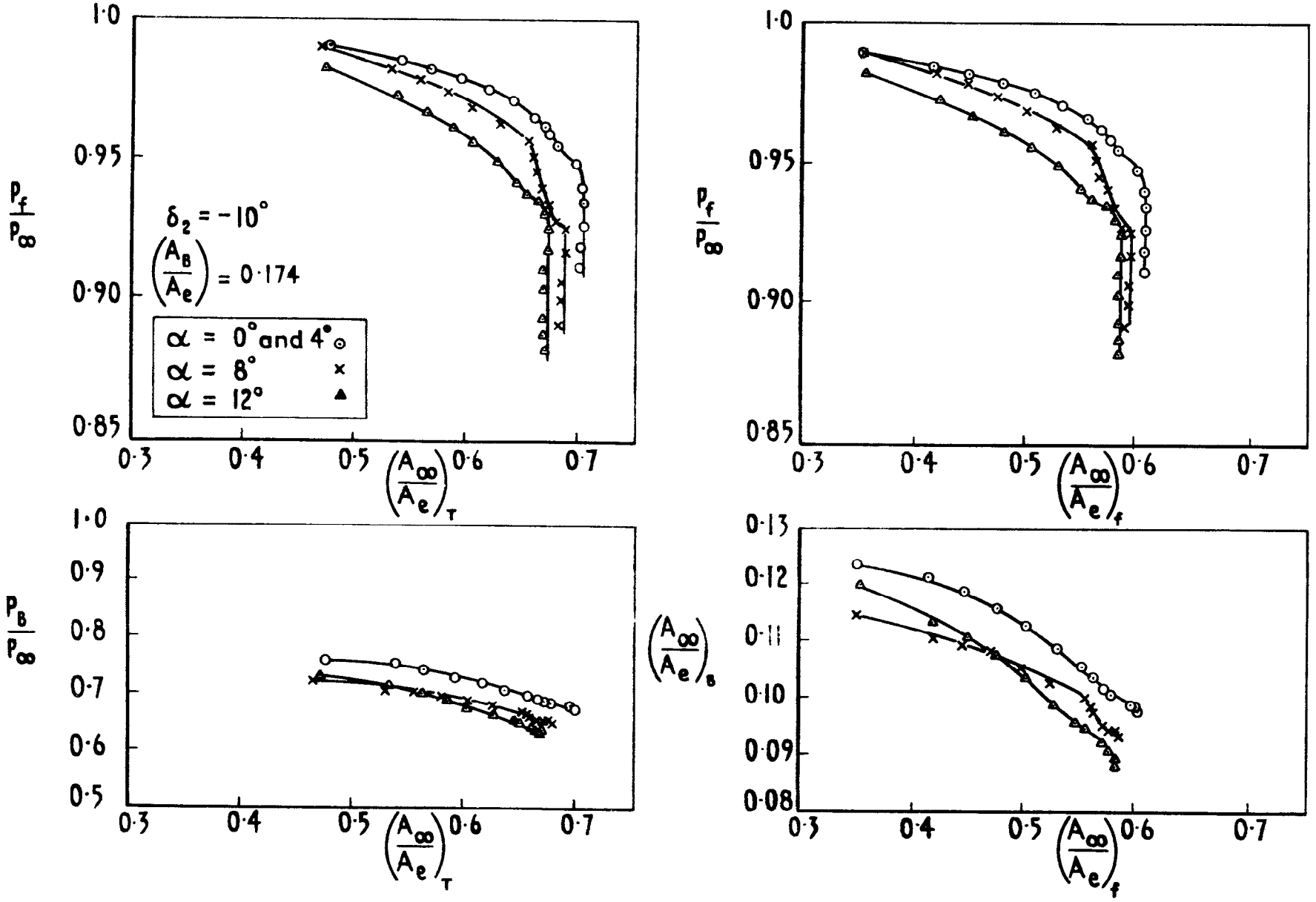

Fig.22 Variation of pressure recovery with mass flow.
Intake with unswept endwalls on fuselage with L E vertical

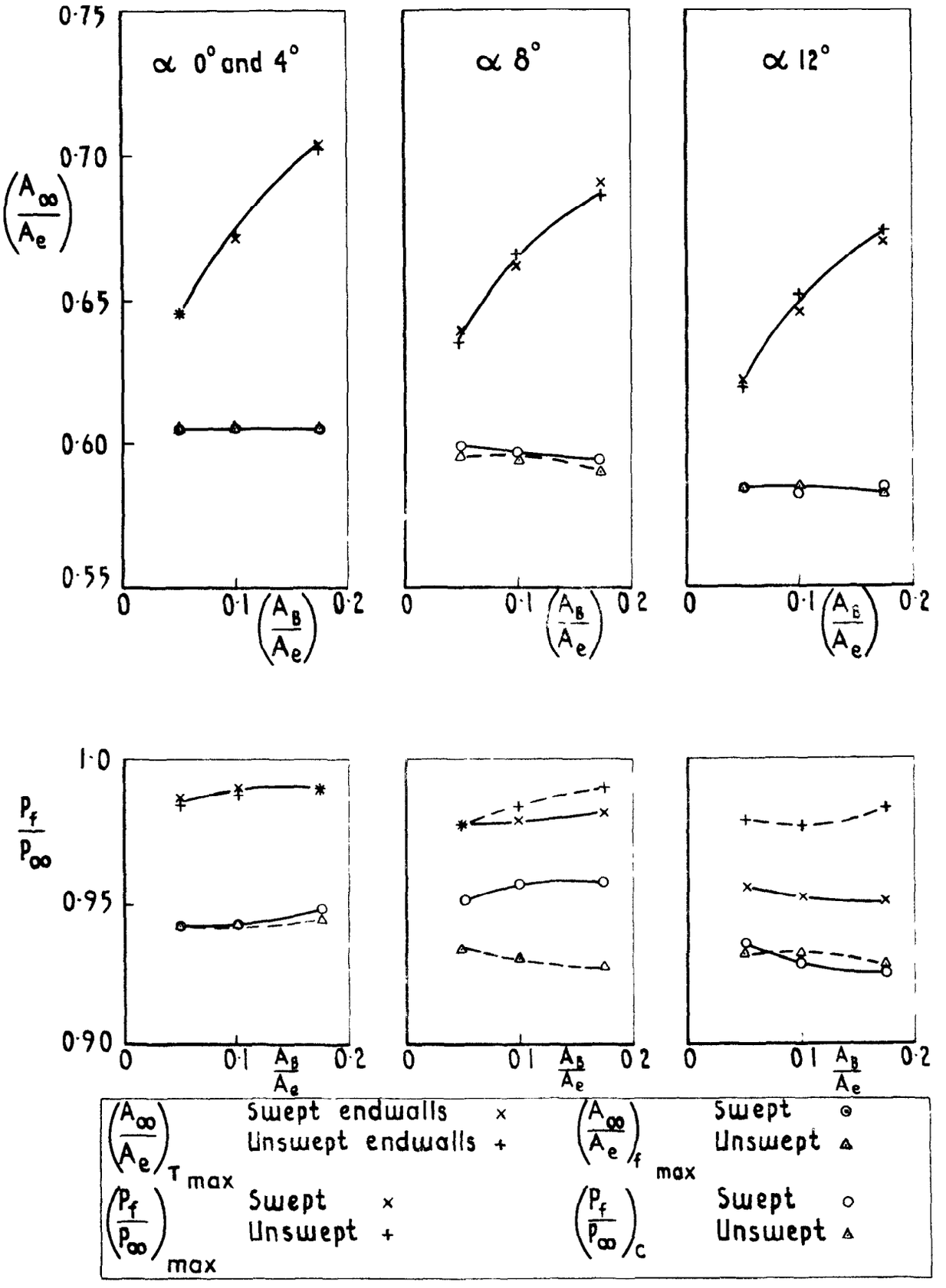

Fig.23 Variation of mass flow and pressure recovery with bleed exit area.
Intake on fuselage. LE vertical. $\delta_2 = -10°$

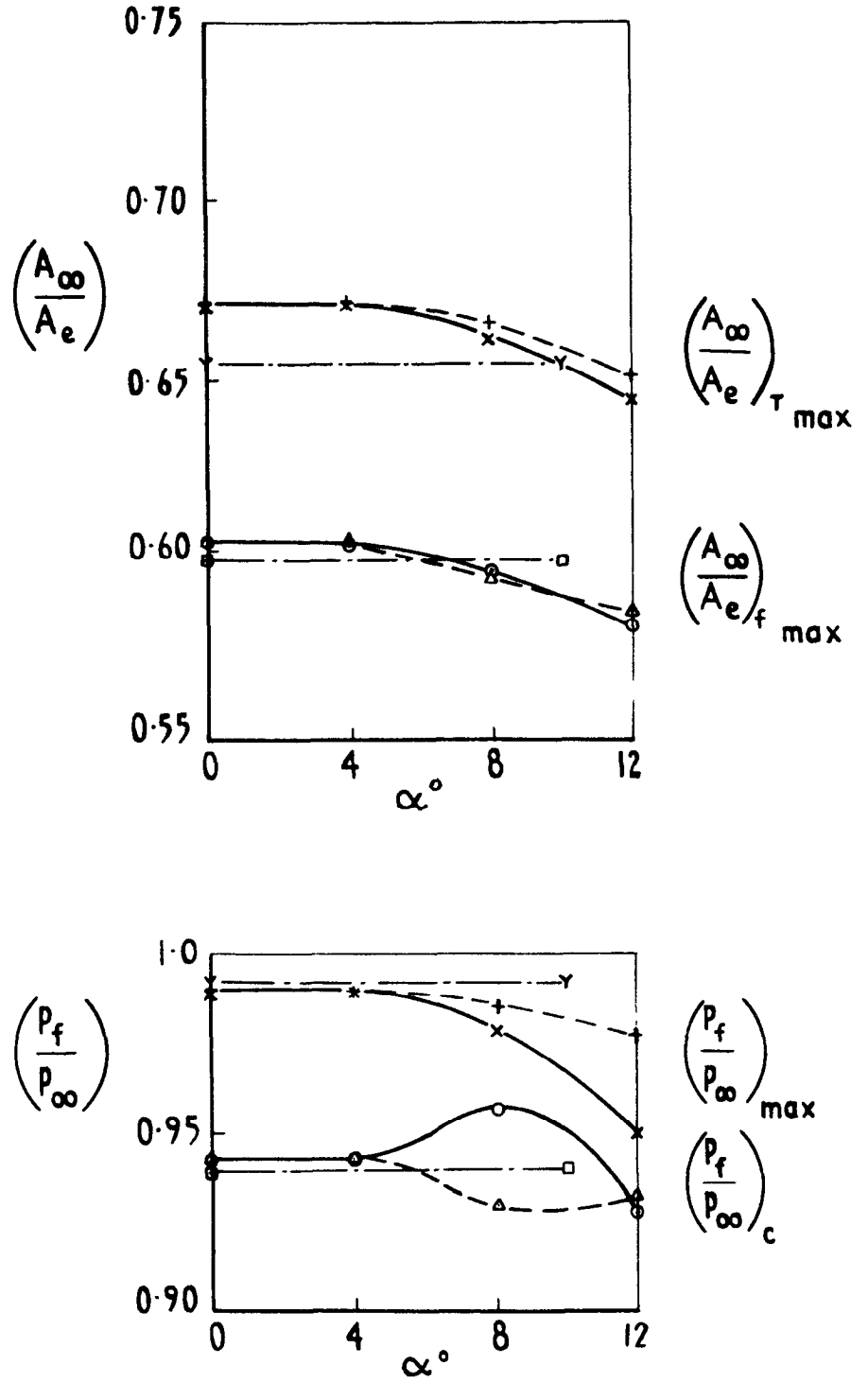

Fig.24 Comparison of mass flow and pressure recovery. Intake on fuselage with L E horizontal and vertical. $\delta_2 = -10^\circ$ $\left(\frac{A_B}{A_e}\right) = 0 \cdot 10$

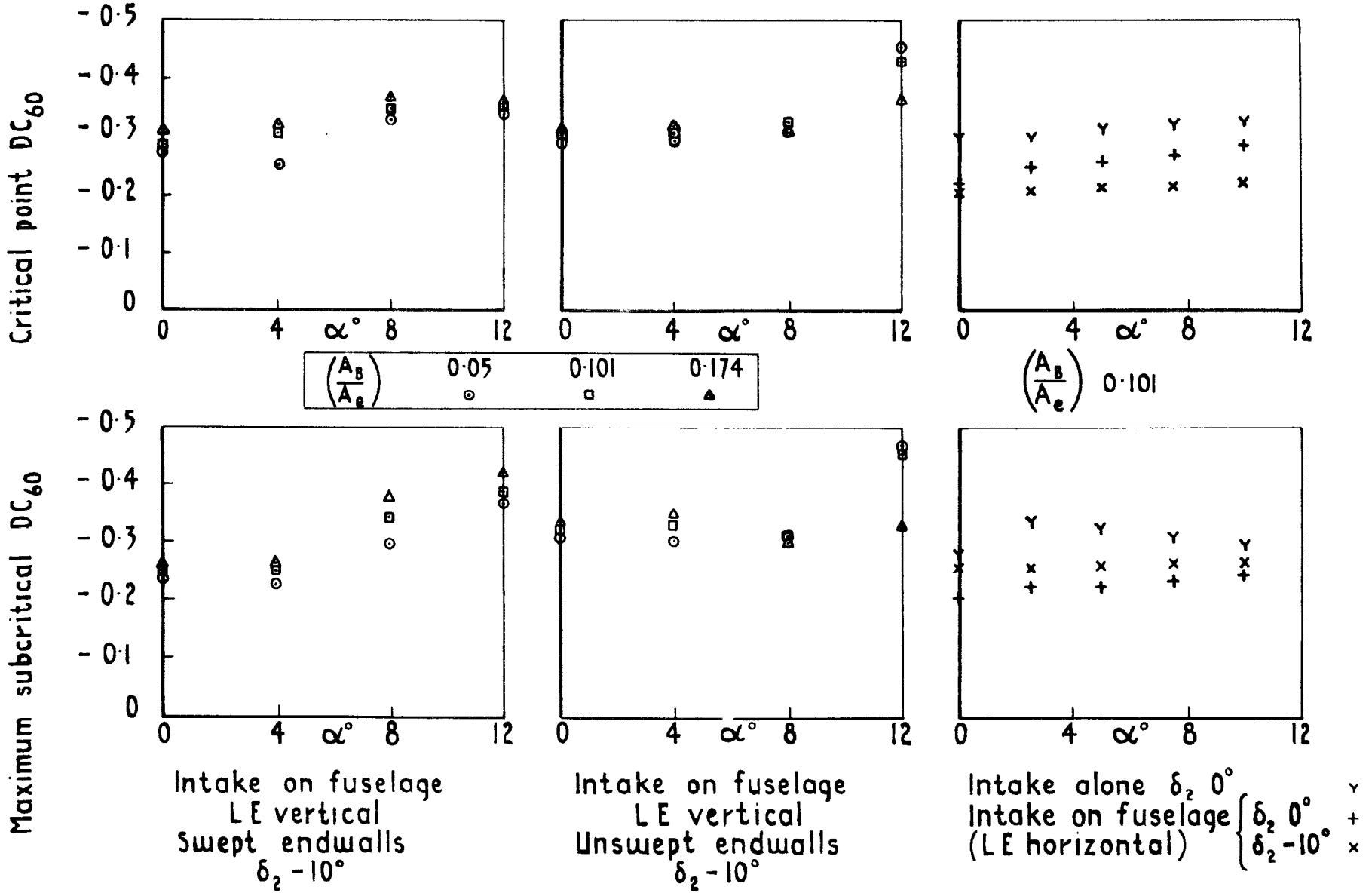

Fig. 25 Engine face distortion coefficient

Printed in England for Her Majesty's Stationery Office by the Royal Aircraft Establishment, Farnborough. Dd. 289030 K3 3/76.

ARC CP No.1346
January 1973

533.697.24 :
532.542.1 ·
533.6 011.35

Brown, C. S.
Goldsmith, E. L.

MEASUREMENT OF THE INTERNAL PERFORMANCE OF A RECTANGULAR AIR-INTAKE AT A MACH NUMBER OF 0.9

A rectangular intake having variable geometry compression surfaces and designed for supersonic operation has been tested at a Mach number of 0 9 and a Reynolds number based on intake entry height of approximately 10^6. Tests have been made on the intake in isolation and on the side of a fuselage.

Maximum mass flow is less than estimates based on geometric throat size. The deficit corresponds to an effective reduction in throat area of about 3 per cent Critical point pressure recovery is lower than predicted, but the difference can be related to a 'turning loss' factor as was the case at supersonic speeds.

(Over)

ARC CP No.1346
January 1973

533.697 24 .
532.542.1 :
533.6.011.35

Brown, C. S.
Goldsmith, E. L.

MEASUREMENT OF THE INTERNAL PERFORMANCE OF A RECTANGULAR AIR-INTAKE AT A MACH NUMBER OF 0.9

A rectangular intake having variable geometry compression surfaces and designed for supersonic operation has been tested at a Mach number of 0.9 and a Reynolds number based on intake entry height of approximately 10^6. Tests have been made on the intake in isolation and on the side of a fuselage.

Maximum mass flow is less than estimates based on geometric throat size. The deficit corresponds to an effective reduction in throat area of about 3 per cent. Critical point pressure recovery is lower than predicted, but the difference can be related to a 'turning loss' factor as was the case at supersonic speeds.

(Over)

DETACHABLE ABSTRACT CARDS

ARC CP No.1346
January 1973

533.697.24 :
532.542 1 .
533.6 011.35

Brown, C S
Goldsmith, E L.

MEASUREMENT OF THE INTERNAL PERFORMANCE OF A RECTANGULAR AIR-INTAKE AT A MACH NUMBER OF 0.9

A rectangular intake having variable geometry compression surfaces and designed for supersonic operation has been tested at a Mach number of 0.9 and a Reynolds number based on intake entry height of approximately 10^6. Tests have been made on the intake in isolation and on the side of a fuselage

Maximum mass flow is less than estimates based on geometric throat size. The deficit corresponds to an effective reduction in throat area of about 3 per cent Critical point pressure recovery is lower than predicted, but the difference can be related to a 'turning loss' factor as was the case at supersonic speeds.

(Over)

Cut here

DETACHABLE ABSTRACT CARDS

With the compression surfaces of the intake horizontal, performance was unaffected by angle of incidence within the range 0° to 10° With the compression surfaces vertical however, there was some loss in maximum mass flow and pressure recovery at critical flow conditions at angles of incidence above about 4° This was only partly alleviated by removal of the swept endwalls.

The presence of this particular fuselage imposed no obvious effect on the performance of the intake.

With the compression
angle of incidence wit
however, there was so
flow conditions at ang
removal of the swept e

The presence of this p
the intake.

With the compression
angle of incidence wit
however, there was so
flow conditions at ang
removal of the swept e

The presence of this p
the intake.

1976

Published by
HER MAJESTY'S STATIONERY OFFICE

Government Bookshops
49 High Holborn, London WC1V 6HB
13a Castle Street, Edinburgh EH2 3AR
41 The Hayes, Cardiff CF1 1JW
Brazennose Street, Manchester M60 8AS
Southey House, Wine Street, Bristol BS1 2BQ
258 Broad Street, Birmingham B1 2HE
80 Chichester Street, Belfast BT1 4JY
Government Publications are also available through booksellers

C.P. No. 1346

ISBN 011 470981 5